

https://dspace.org/

The dissolution of a Transvaal chromite in liquid silicate slags under an inert atmosphere at 1550 celcius degrees and 1650 celsius degrees.

Curr, Thomas Robert

1990
https://hdl.handle.net/10539/24333

Downloaded from a DSpace repository. https://dspace.org/

THE DISSOLUTION OF A TRANSVAAL CHROMITE IN LIQUID SILICATE SLAGS UNDER AN INERT ATMOSPHERE AT 1550°C AND 1650°C

THOMAS ROBERT CURR

A dissertation submitted to the Faculty of Engineering, University of the Witwatersrand, in fulfilment of the requirements for the degree of Master of Science in Engineering.

Randburg, 1990

DECLARATION

I declare that this dissertation is my own, unaided work. It is being submitted for the Degree of Master of Science in Engineering in the University of the Witwatersrand, Johannesburg. It has not been submitted before for any degree or examination in any other University. The research was conducted while the author was a full-time employee of the Council for Mineral Technology using the research facilities of the Council.

.....
T.R. CURR

this 2nd. day of MAY..., 1990

ABSTRACT

The role of chromite dissolution in the smelting of ferrochromium was investigated with the object of improving the throughput and chromium recovery of the process. The solubility of a typical Transvaal chromite in silicate slags with CaO/SiO_2 ratios from 0,03 to 0,55 at 1550°C and 1650°C was determined. Synthetic slags were melted in porous chromite crucibles and the slag underwent repeated reactions with the chromite grains as it penetrated the crucible wall. Finally the slag came into equilibrium with the original chromite towards the outer part of the crucible wall. Microprobe analysis of this slag yielded the maximum or saturated solubilities of the chromite constituents in the slag.

The solubility of Cr_2O_3 was found to be low (~1 per cent) while the remaining components' solubilities (Al_2O_3 ~16 per cent, $FeO)_t$ ~12 per cent and MgO ~8 per cent) were significantly higher. CaO/SiO_2 ratios greater than 0,1 lowered the solubility of MgO significantly (e.g. from 14,1 per cent to 5,8 per cent at 1650°C).

The complete dissolution of this chromite in these slags requires the slag to contain less than the solubility limits of each of these species simultaneously. It was recommended that the best way to achieve this in practice would be a well-stirred slag bath containing suspended carbon particles, in which a CaO/SiO_2 ratio of less than 0,1 was maintained. Further work to investigate the effect of slag composition (including Na_2O and CaF_2) on the kinetics of chromite reduction in such a system was recommended.

To my wife, Claire

ACKNOWLEDGEMENTS

The financial support provided by the Council for Mineral Technology (Mintek) is gratefully acknowledged as is the permission of Mintek to publish this dissertation.

The assistance provided by the Mineralogy and Analytical Science Divisions at Mintek in analysing the samples and the provision of facilities and equipment by the Pyrometallurgy Division at Mintek is gratefully acknowledged.

Contents

1 INTRODUCTION 1

1.1 The Submerged-arc Furnace 3

1.2 New Processes 4

2 CHROMITE SMELTING 5

2.1 Chromite Composition and Structure . . 6

2.2 Reduction Reactions 9

2.3 Reduction Mechanism 13

2.4 Chromite dissolution 16

3 EXPERIMENTAL PLANNING 19

3.1 Objectives and Scope 19

3.2 Prior Work 20

3.3 Design of Experiments 22

4 EXPERIMENTAL WORK 26

4.1 Preparation of Materials 26

4.1.1 Chromite crucibles 26

4.1.2 Master slags 32

4.2 Description of Apparatus 36

4.3 Experimental Method 38

5 RESULTS 43

6 DISCUSSION 50

6.1 The Porous Crucible Technique 50

6.2 The Effects of Temperature and CaO/SiO_2 Ratio 57

6.3 Implications for Chromite Smelting . . 62

7 CONCLUSIONS 65

8 RECOMMENDATIONS 67

Contents (continued)

9. APPENDICIES 69

APPENDIX 1. Calculation of the activities of various chromium oxide compounds in equilibrium with Fe-Cr-C and Fe-Cr-Si alloys 69

APPENDIX 2. Details of the experimental equipment 73

Figure A-1. Schematic diagram of the vertical tube furnace facility 76

Figure A-2. Location of the crucible in the furnace 77

Figure A-3. Resistivity of molybdenum 78

Figure A-4. Molybdenum heating element, winding pattern 79

APPENDIX 3. Calibration of reference thermocouple 80

Figure A-5. Comparison of calibrated thermocouple with American National Standard data 83

APPENDIX 4. Details of the experimental test runs 85

Table A-1 - Details of test runs at 1550°C 88

Table A-2 - Details of test runs at 1650°C 88

APPENDIX 5. Detailed results of micro-analyses 89

Table A-3. Detailed results of microanalyses for each run 90

10. REFERENCES 105

Tables

Table 1: Composition of chromite ores, after Healy[12] 7

Table 2: Equilibrium activities of Cr_2O_3, CrO and $MgCr_2O_4$ in slags in contact with Fe-Cr-C alloys 12

Table 3: Equilibrium activities of Cr_2O_3, CrO and $MgCr_2O_4$ in slags in contact with Fe-Cr-Si alloys 13

Table 4: Effect of dissolution on chromite composition after Roos[36] (mass %) . . . 23

Table 5: Winterveld chromite fractions after gangue removal 28

Table 6: Parameters used in the preparation of chromite crucibles 31

Table 7: Composition of chromite and a sintered chromite crucible 32

Table 8: Particle size distribution of the chromite 32

Table 9: Preparation of master slags 34

Table 10: Chemical analyses of master slags . . . 36

Table 11: Summary of final test runs 43

Table 12: Significance of the concentration gradients measured in chromite grains from the outer part of the crucible wall . . 47

Table 13: Effect of slag on chromite composition at equilibrium 49

Table 14: Chromite saturated slag compositions . 50
Table 15: Comparison of initial and final slag compositions 56
Table 16: Compositions of the edges of chromite grains from the crucible inner wall . . 56
Table 17: Activity coefficients of MgO, Al_2O_3, $(FeO)_T$ and Cr_2O_3 in chromite saturated slags . 62

Figures

Figure 1: Schematic arrangements of chromite smelting furnaces 2
Figure 2: Smelting reduction mechanism after Fukagawa and Shimoda[33] 15
Figure 3: Possible concentration gradients of Cr_2O_3 in a chromite-slag-metal-carbon system .18
Figure 4: Chromite crucible 29
Figure 5: 100 kVA graphite crucible plasma furnace 34
Figure 6: Composition of the master slags as the pseudeo-ternary (SiO_2 + CaO)-MgO-Al_2O_3 .36
Figure 7: Schematic arrangement of vertical tube furnace 37
Figure 8: Arrangement of crucible and thermocouple 39
Figure 9: Typical appearance of chromite grains near the inner and outer surfaces of the crucible wall after slag contact . . . 44
Figure 10: Comparison of the CaO/SiO_2 ratios of the master and equilibrium slags 51
Figure 11: Composition of slags in equilibrium with chromite at 1550 °C 52
Figure 12: Composition of slags in equilibrium with chromite at 1650 °C 53

LIST OF SYMBOLS

		Units
a_i	Activity of species i (mole fraction relative to pure species at system temperatures)	-
$C^{o}_{Cr_2O_3}$	Molar concentration of Cr_2O_3 at slag-metal interface	$mole.m^{-3}$
$C^{\infty}_{Cr_2O_3}$	Molar concentration of Cr_2O_3 in bulk slags	$mole.m^{-3}$
$C^{s}_{Cr_2O_3}$	Saturation molar concentration of Cr_2O_3	$mole.m^{-3}$
i(g)	Denotes gaseous species i	-
i(l)	Denotes liquid species i	-
i(s)	Denotes solid species i	-
$\underline{i}$	Denotes species i dissolved in liquid metal phase	-
(i)	Denotes species i dissolved in liquid slag phase	-
[i]	Denotes species i dissolved in solid solution	-
k_M	Mass transfer coefficient	$m.s^{-1}$
$(FeO)_T$	Denotes total iron expressed as FeO	mass %
$N^{o}_{Cr_2O_3}$	Molar flux of Cr_2O_3 at the slag-metal interface	$mole.m^{-2}.s^{-1}$
P_i	Partial pressure of species i	atmospheres
R	Gas constant	$cal.mole^{-1}.K^{-1}$
T	Temperature	°K
K_j	Equilibrium constant for reaction j	-
X_i	Mole fraction of species i	-
γ_i	Activity coefficient of species i	
γ^{o}_i	Activity coefficient of species i at infinite dilution	-
ΔG^{o}_j	Standard free energy change for reaction j	$cal.mole^{-1}$

Δm	Change in sample mass as a percentage of initial mass	-
ΔT	Maximum-minimum temperatures recorded	°C
e_i^k	Interaction coefficient of species k on species i in dilute iron solution	-
i%	Concentration of species i	mass %
ϕ	Phase	-
Å	Ångström	10^{-10}m
cf.	Compare	-

LIST OF CHEMICAL EQUATIONS

				Page
1.	$FeO_x(s) + xC(s)$	=	$Fe(l) + xCO(g)$	9
2.	$Cr_2O_3(s) + 3C(s)$	=	$2Cr(l) + 3CO(g)$	9
3.	$Fe_3O_4(s) + 4C(s)$	=	$3Fe(l) + 4CO(g)$	9
4.	$FeCr_2O_4(s) + 4C(s)$	=	$2Cr(l) + Fe(l) + 4CO(g)$	9
5.	$MgCr_2O_4(s) + 3C(s)$	=	$2Cr(l) + MgO(s) + 3CO(g)$	9
6.	$(CrO) + \underline{C}$	=	$\underline{Cr} + CO(g)$	11
7.	$\underline{C} + \frac{1}{2}O_2(g)$	=	$CO(g)$	11
8.	$(Cr_2O_3) + \underline{Si}$	=	$(SiO_2) + (CrO) + \underline{Cr}$	16
9.	$2(CrO) + \underline{Si}$	=	$(SiO_2) + 2\underline{Cr}$	16
10.	$(Cr_2O_3) + \underline{Cr}$	=	$3(CrO)$	17
11.	$1,5\underline{Si} + (Cr_2O_3)$	=	$2\underline{Cr} + 1,5(SiO_2)$	71
12.	$0,5\underline{Si} + (CrO)$	=	$\underline{Cr} + 0,5(SiO_2)$	71
13.	$1,5\underline{Si} + [MgCr_2O_4]$	=	$2\underline{Cr} + (MgO) + 1,5(SiO_2)$	71
14.	$\underline{Si} + O_2(g)$	=	(SiO_2)	71

1 INTRODUCTION

Stainless steels have become widely accepted materials in both the industrial and the consumer markets since their discovery in 1912[1]. The world-wide consumption of stainless steel has grown at more than 3 per cent per annum since 1960 when large-scale production methods became available[2]. Ferrochromium is an intermediate alloy used for the production of stainless steel and is the ultimate source of all the chromium contained in the final steel (typically 18 per cent chromium). Ferrochromium is, in turn, produced from chromite, the only commercially significant chromium ore. The majority of the ferrochromium produced is designated high-carbon ferrochromium and contains typically 6 to 8 per cent carbon and 50 to 65 per cent chromium.

The production of this alloy is usually carried out in submerged-arc electric smelting furnaces[3] from chromite, a carbonaceous reducing agent and fluxes. The use of plasma furnace technology for this purpose has recently become an industrial reality[4] and several new processes, based on pneumatic steel making technology in a converter, are under development[5]. All these processes yield liquid slag and liquid high-carbon ferrochromium together with carbon monoxide gas as the major reaction products and are energy-intensive processes because of the high temperatures of the liquid products (>1650°C) and the strongly endothermic reduction reactions. The processes differ, however, in the manner in which the energy and feed materials are introduced into the reaction zone (see Figure 1) and a brief description of the major features of these units is necessary here to define the role of chromite dissolution in ferrochromium production.

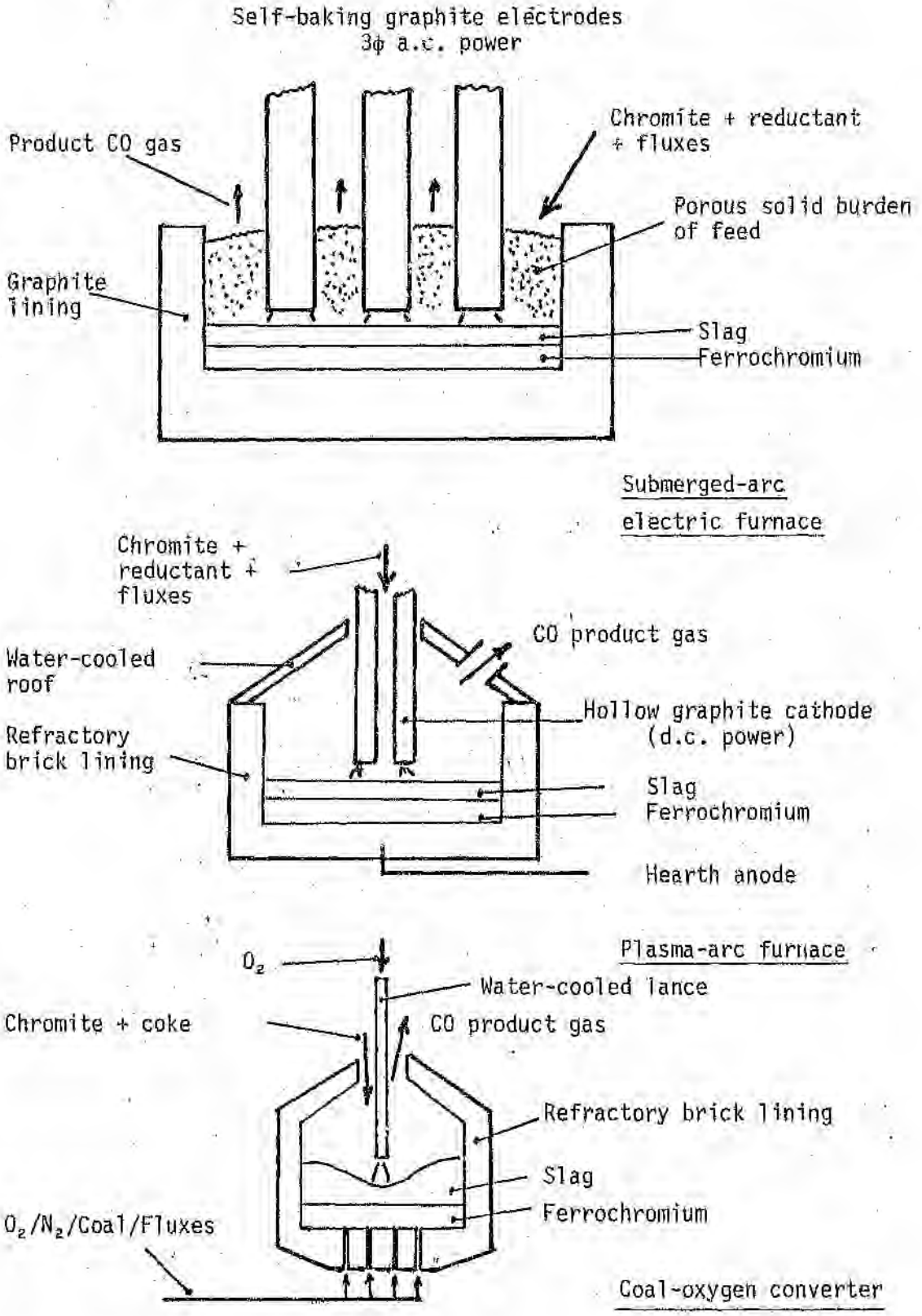


Figure 1. Schematic arrangements of chromite smelting furnaces

1.1 The Submerged-arc Furnace

This furnace usually consists of a carbon-lined circular steel shell containing three vertical graphite electrodes submerged in a burden of solid raw material. Alternating current electric power supplied to the electrodes creates a high temperature smelting zone beneath the tips of the electrodes into which raw materials fall and away from which molten slag and metal run to collect in the hearth. The off-gases pass upwards through the permeable burden of raw material which is thereby pre-heated. The slag and metal are removed intermittently from the hearth by tapping the furnace while a choke-type feed system maintains a constant level of raw materials around the electrodes.

An examination of the discard slags from submerged-arc furnaces at three different ferro-alloy plants by Oosthuyzen and Viljoen[6] has shown that when pre-reduced chromite pellets are used as the feed material the total chromium content (i.e. oxides plus metallics expressed as chromium) of the slag was as low as 4,4 per cent while, when briquetted chromite or unagglomerated chromite fines were used, the slag contained between 14,6 per cent and 16,5 per cent chromium. South African reserves of chromite are extensive[7] (81 per cent of world reserves) but over 70 per cent of these ores are friable[7] and only a relatively small proportion of South Africa's production capacity uses the pelletized pre-reduction of chromite route[7]. The loss of chromium to the discard slag is, therefore, a significant factor in the production of ferrochromium from Transvaal chromites in South Africa. The high chromium contents of discard slags (14,6 to 16,5 per cent) results in a low recovery of the input chromium to the ferrochromium alloy, typically less than 75 per cent.

Oosthuyzen and Viljoen[6] also determined that more than 60 per cent of the chromium present in the high chromium content discard slags was 'contained in undissolved and partly altered chromite particles'. It was also found that the slag sample with a low chromium content (4,4 per cent) had virtually no undissolved and partly altered chromite particles present. The presence of undissolved chromite particles in the slags from submerged-arc furnaces is therefore associated with poor chromium recoveries and an understanding of the mechanism of the dissolution process may well be of importance.

1.2 New Processes

The South African plasma smelting process for chromite[4] uses a refractory-lined steel shell with a single graphite electrode located centrally. An electrically conductive hearth is used to complete a direct current path consisting of the graphite electrode, the plasma arc, the molten bath of slag and metal and the furnace hearth (see Figure 1). The process is an open-bath type and no burden of solid raw material exists above the molten bath. The requirements for a sufficiently permeable burden, to allow the release of the reaction gases, falls away thereby allowing the direct use of chromite ore fines. The pilot-scale testwork by Barcza, et al.[8] showed that slags with low levels of chromium (< 3 per cent) could be produced despite the unagglomerated nature of the chromite. It was found, however, that in cases where poor recoveries of chromium to the metal were obtained, that the slag contained large numbers of undissolved and partly altered chromite particles.

The new processes based on a converter[5,9,10] utilize coal - oxygen combustion - to provide the energy and solids injection

technology to introduce various combinations of chromite/coke/coal/fluxes into the metal bath and/or top charging chromite/coke/fluxes as well as using an oxygen top lance[10] (see Figure 1). There is again no solid burden present above the molten slag/metal bath and final slags with low chromium contents are attainable (<1 per cent chromium)[5]. The form of the chromium in the slag was reported[9] as consisting primarily of oxides of chromium in solid particles whenever the total chromium content of the slag exceeds 4 per cent.

The dissolution rate of the chromite and the solubility of chromium in the slag were considered by Enokido, et al.[9] as controlling the reaction rate as long as chromite particles remained suspended in the slag.

The two new types of processes for ferrochromium production both introduce the chromite directly into a molten slag/metal bath and virtually all the chromium lost to the slag above the 3 to 4 per cent total chromium content level consisted of undissolved chromite particles. This form of loss also occurred in the submerged-arc furnace practice. The dissolution of chromite therefore appears likely to play a significant role in the reduction of chromite to ferrochromium whenever a liquid slag forms part of the smelting process. An examination of the current status of knowledge on the smelting of chromite is therefore presented in the following section.

2 CHROMITE SMELTING

The carbothermic smelting of chromite is carried out[3] by the addition of fluxes and reducing agents (typically quartz, dolomite, limestone, serpentine, char and coke) to form silicate slags and ferrochromium. The final slags formed, if

good recoveries of chromium are achieved contain less than 3 per cent by mass of Cr_2O_3 + "FeO," and can then be adequately described by the system SiO_2-CaO-MgO-Al_2O_3 for which well established phase diagrams are available[11]. The smelting process itself on the other hand involves the slag system FeO_x-CrC_y-SiO_2-CaO-MgO-Al_2O_3 (where x and y are variable between 0,95 and 1,5) for which no complete phase diagrams are available. The complete smelting system also involves at least three other phases; solid carbon, liquid metal (Fe-Cr-C-Si) and a gas (principally carbon monoxide). The presence of at least two phases in the slag, solid chromite and a liquid silicate melt should also be included as discussed earlier. This highly complex process is discussed here in three sub-sections for clarity; the principal raw material chromite, the most applicable reduction reactions and finally some likely reaction mechanisms in which the rate of chromite dissolution will be examined.

2.1 Chromite Composition and Structure

Chromite ores and concentrates consist of a chromium containing spinel and relatively small amounts of gangue minerals, usually magnesium silicates[12]. These ores are variable in composition, particularly with regard to their Cr/Fe ratio, chromium content and MgO/Al_2O_3 ratio. Healy[12] has listed a range of chromites that illustrate this variability (see Table 1). The subject of chromite spinels has been comprehensively treated by Ulmer[13] and some of the information which was considered most relevant to the chromite smelting process is reproduced here.

Table 1: Composition of chromite ores, after Healy[12]

Chromite ore	Composition (mass, %)						
	Cr_2O_3	Al_2O_3	$(FeO)_T$	MgO	SiO_2	Cr/Fe	MgO/Al_2O_3
Transvaal	44,5	15,5	24,7	10,1	2,2	1,59	0,65
Dyke	49,2	11,4	18,3	12,4	6,6	2,37	1,09
Turkish	48,5	10,0	13,3	18,8	6,9	3,25	1,88
Masinloc	32,1	30,2	12,7	18,1	5,0	2,22	0,60

The general formula for the oxide chromite spinels is AB_2O_4 where A is divalent iron or magnesium, B is trivalent iron, chromium or aluminium and O is oxygen. The unit cell is expressed as $A_8B_{16}O_{32}$ in which the 32 oxygen anions are cubic close-packed to provide 64 tetrahedrally co-ordinated cation sites and 32 octahedrally co-ordinated cation sites. The 32 anions and 24 cations form a face-centered unit cell with an approximate cell edge length of from 8,0 to 8,4 Å depending on the cations involved. The chromite spinels show almost complete solid solution among the six end-members ($FeFe_2O_4$, $MgFe_2O_4$, $FeAl_2O_4$, $MgAl_2O_4$, $FeCr_2O_4$ and $MgCr_2O_4$) at temperatures above 1000°C. The large number of unfilled cation sites in the unit cell allows for different arrangements of the cations of which two extreme arrangements have been recognized. The ideal normal spinel where the trivalent cations occupy only octahedral sites and the divalent cations occupy only tetrahedral sites and the ideal inverse spinel where half of the trivalent cations and all of the divalent cations occupy octahedral sites while the remaining trivalent cations occupy tetrahedral sites. The distribution of cations between

tetrahedral and octahedral sites has been discussed by Burns[14] in terms of the crystal field theory to explain the dominance of Cr^{3+} ions in octahedral co-ordination.

The crystal field stabilization energy resulting from tetrahedral coordination of Cr^{3+} would amount to less than 30 per cent of that resulting from octahedral coordination, hence the large octahedral site preference energy for Cr^{3+} of 16,6 kcal/mole as given by Ulmer[13]. The values of this parameter for the other chromite spinel cations define the following increasing order of octahedral site preference: Fe^{3+}(-13,3), Fe^{2+}(-9,9), Mg^{2+}(-5,0), Al^{3+}(-2,5) and Cr^{3+}(+16,6) with the respective energies given in parentheses. Ulmer[15] in discussing the work of Datta[16] pointed out, however, that for the case of $MgAl_2O_4$ that the cation coordination changes with the temperature of preparation of the compound and therefore even in a relatively simple end-member of the chromite spinels that 'an exact assignment of the 24 cations to the 96 possible cation sites is an irresolvable problem'. The complexity of chromite spinels has been further highlighted by Stubican and Greskovich[17] who demonstrated that a spinel with 3,05 Cr^{2+} cations per unit cell in tetrahedral coordination could be prepared from mixtures of MgO and Cr_2O_3 heated under reducing conditions at between 1800°C and 2000°C. The cation coordination can therefore be seen to be affected by the temperature and reducing conditions at which the chromite spinel was formed and presumably similar changes in cation coordination could be expected during the high temperature reduction process. This phenomenon could have a significant bearing on the reduction behaviour of chromites.

2.2 Reduction Reactions

The simplest treatment of chromite reduction assumes reduction of the simple oxides of iron and chromium to metal and carbon monoxide as follows:

$$FeO_x(s) + xC(s) = Fe(l) + xCO(g) \quad ....(1)$$

$$Cr_2O_3(s) + 3C(s) = 2Cr(l) + 3CO(g) \quad ....(2)$$

This basic approach has been used successfully for mass and energy balances on large furnaces[18] with minor corrections for the observed presence of carbon and silicon in the high-carbon ferrochromium alloys produced in practice. This method, while highly effective for monitoring and controlling the metallurgical performance of a smelting furnace, is clearly not useful as a basis for calculating the expected losses of chromium to the slag when these are in the form of chromite spinels.

Healy[12] has recently utilized the thermodynamic data available for the chromite spinel end-members $MgCr_2O_4$, Fe_3O_4, $MgAl_2O_4$ and $FeCr_2O_4$ to predict the smelting behaviour of chromites as a function of the temperature of reaction and the degree of reduction achieved. The relevant equations used were:

$$Fe_3O_4(s) + 4C(s) = 3Fe(l) + 4CO(g) \quad ....(3)$$

$$FeCr_2O_4(s) + 4C(s) = 2Cr(l) + Fe(l) + 4CO(g) \quad ....(4)$$

$$MgCr_2O_4(s) + 3C(s) = 2Cr(l) + MgO(s) + 3CO(g) \quad ....(5)$$

Healy[12] has used this method to investigate the effects of chromite composition upon the carbon contents of the alloys required to achieve a desired chromium recovery at a fixed temperature. This theoretical approach was shown by Healy to agree well with submerged-arc furnace practice, where chromites with high Cr/Fe ratios and high MgO/Al_2O_3 ratios are

known[12] to produce alloys with lower carbon contents. This method does not, however, consider the possible role of CrO in the reduction process although Rankin and Biswas[19], Maeda and Sano[20] and Muan[21] have all found that chromium exists in silicate slags under reducing conditions, predominantly in the divalent form. Earlier work by Korber and Oelsen[22] in 1935 and Esin and Zakharov[23] in 1958 came to the same conclusion. Muan[21] has shown that a large increase (30 per cent cf. 2 per cent) in the solubility of chromium (as CrO) but expressed as Cr_2O_3 in the SiO_2-MgO-Cr_2O_3 system occurs when the system is in contact with metallic chromium rather than air. Rankin and Biswas[19] equilibrated slags at 1600°C with CaO/SiO_2 ratios from 0,27 to 2,1 with metals containing from 5 to 30 per cent chromium and up to 2,5 per cent silicon. These slags were usually glassy in nature and blue in colour at room temperature and contained up to 25,6 per cent chromium. These slag-metal equilibrium studies[19,21] in the absence of carbon differ greatly in slag chromium content from the work of Maeda and Sano[20] in which graphite crucibles and carbon saturated metals were used. The chromium contents of these slags lay in the range 10 to 200 p.p.m. at 1650°C and were also considered to be present in the slag as CrO.

The possible forms in which chromium may be lost to the slag can therefore include; undissolved partly reacted chromite particles, dissolved Cr_2O_3 and CrO in the silicate phase, chromite spinel recrystallized from the silicate phase and entrained metallic blebs. An estimate of the relative magnitudes of these forms of loss at equilibrium was undertaken using thermodynamic data from Barin and Knacke[24] and Toker[25] to calculate the equilibrium constants for the

following reactions at 1600°C, under one atmosphere of carbon monoxide.

$$(Cr_2O_3) + 3\underline{C} = 2\underline{Cr} + 3CO(g) \quad \ldots.(2)$$

$$(CrO) + \underline{C} = \underline{Cr} + CO(g) \quad \ldots.(6)$$

$$[MgCr_2O_4] + 3\underline{C} = 2\underline{Cr} + 3CO(g) + (MgO) \quad \ldots.(5)$$

where ( ) denotes solution in a liquid silicate slag

[ ] denotes solid solution in a chromite spinel

and $\underline{C}$, $\underline{Cr}$ denotes solution in a liquid Fe-Cr-C alloy.

The activities of the carbon and chromium in the metal phase were estimated from the graphs presented by Healy[26] in a recent paper. The activities of Cr_2O_3, CrO and $MgCr_2O_4$ were calculated (see Appendix I) as a function of the carbon content of the metal which was related to the oxygen partial pressure in the system under consideration by the reaction

$$\underline{C} + \tfrac{1}{2}O_2 = CO \quad \ldots.(7)$$

where $\underline{C}$ denotes carbon dissolved in the metal as before.

The results, shown in Table 2, demonstrate the wide range of reducing conditions (i.e. P_{O_2} ranging from $1,4 \times 10^{-15}$ atm. to $4,8 \times 10^{-11}$ atm.) defined by a relatively small range of carbon contents (8,0 to 1,0 mass per cent) in the Fe-Cr-C alloy. This is reflected in the wide range of carbon activities (0,56 to 0,003) and of interest is the strong effect of carbon content upon the chromium activities (0,09 to 0,40) at a constant chromium content in the alloy of 50 mass per cent).

Table 2: Equilibrium activities of Cr_2O_3, CrO and $MgCr_2O_4$ in slags in contact with Fe-Cr-C alloys

Alloy			Atmosphere	Slag activities		
C mass %	a_C	a_{Cr}	pO_2 atm	Cr_2O_3	CrO	$MgCr_2O_4$
8,0	0,56	0,09	$1,39 \times 10^{-15}$	$3,48 \times 10^{-7}$	$3,2 \times 10^{-3}$	$4,69 \times 10^{-6}$
4,0	0,076	0,24	$7,53 \times 10^{-14}$	$9,90 \times 10^{-4}$	$6,41 \times 10^{-2}$	$1,34 \times 10^{-2}$
1,0	0,003	0,40	$4,84 \times 10^{-11}$	Saturated	Saturated	Saturated

Notes: (1) All activities relative to pure species at 1600°C

(2) Constant conditions : 50 mass per cent Cr in the alloy
: MgO activity in the slag = 0,17
: Pressure = 1 atm., p_{CO} = 1 atm.
Temperature = 1600°C

The activities of the chromium oxides in equilibrium with these alloys indicate that CrO would be the predominant oxide form at 8 per cent carbon in the alloy while $MgCr_2O_4$ and CrO would be approximately equal at 4 per cent carbon and all oxide forms would be stable at unit activities before the alloy carbon content dropped as low as 1 per cent. A similar pattern emerges if Fe-Cr-Si alloys are considered with silicon contents from 5,0 to 0,05 mass per cent and associated oxygen partial pressures between 2×10^{-14} and 2×10^{-11} atmospheres (see Table 3). This would indicate that the activity coefficient of CrO (γ_{CrO}) in the system studied by Rankin and Biswas[19] was approximately unity for slag chromium contents from 1 to 25 per cent, which is similar to that reported by Muan[21] in a comparison with the behaviour of FeO in $CaO-SiO_2$ slag systems. Maeda and Sano[20], however, report values for γ_{CrO} ranging from 30 to 300 but these were determined for very low chromium concentrations in the slag, i.e. 10 to 200 p.p.m.

Table 3: Equilibrium activities of Cr_2O_3, CrO and $MgCr_2O_4$ in slags in contact with Fe-Cr-Si alloys

Alloy		Atmosphere	Slag activities		
Si mass %	a_{Si}	pO_2 atm	Cr_2O_3	CrO	$MgCr_2O_4$
5,0	$1,34 \times 10^{-3}$	$2,53 \times 10^{-18}$	$7,00 \times 10^{-4}$	0,065	0,013
0,5	$1,85 \times 10^{-5}$	$1,84 \times 10^{-12}$	0,431	0,529	Saturated
0,05	$1,48 \times 10^{-6}$	$2,29 \times 10^{-11}$	Saturated	Saturated	Saturated

Notes: (1) All activities relate to pure species at 1600°C

(2) Constants: activity of Cr in alloy = 0,4;
activity of MgO in slag = 0,17;
activity of SiO_2 in slag = 0,4;
Pressure = 1 atm. (inert)
Temperature = 1600°C

It can be seen, therefore that, if reducing conditions in the smelting reduction of chromite are not maintained by the presence of either solid carbon or metal with more than 4 per cent carbon (or 5 per cent silicon), that losses of chromium to the slag can be expected both via CrO and $MgCr_2O_4$. The loss as $MgCr_2O_4$ contained within a solid chromite spinel is more likely to be enhanced by kinetic factors especially the dissolution step which will be discussed in the following section.

2.3 Reduction Mechanism

The reaction mechanisms for the smelting of chromite (i.e. in the presence of a liquid slag phase) have not been extensively studied, unlike solid-state reduction which has been the subject of numerous investigations[27-30] at the University of the Witwatersrand. Solid-state reduction can be carried out at temperatures as low as 1300°C in less than 2 hours, using

gangue-free Transvaal chromite and graphite[30]. The iron was virtually completely reduced to metal while approximately 70 per cent of the chromium was reduced. The metal forms on the chromite surface and Algie and Finn[30] found that when the extent of total reduction (of the chromium and iron oxides) was less than 50 per cent that the rate was controlled by a variety of different processes (carbon monoxide formation, metal nucleation and metal carburization) which were inherently variable, i.e. non-reproducible. The reduction rate was, however, found to be controlled in a reproducible fashion - above 50 per cent reduction, by solid-state diffusion of chromium ions in the chromite spinel to the outer metal product layer. Urquhart[31] simulated the smelting behaviour of the burden in submerged-arc furnaces in a series of induction furnace tests at fixed temperatures and concluded that for solid-state reduction the rate-limiting step was the diffusion of iron and chromium ions in the spinel. The rate of reduction was found to have increased when a slag formed at temperatures above 1500°C. Dawson and Edwards[32] have shown that the addition of sodium and calcium fluoride to flux a mixture of chromite and graphite produces almost complete (~90 per cent) reduction at 1300°C within two hours, whereas in the absence of these fluxes only 70 per cent reduction occurred after four hours. The metal formed predominantly at the surface of the carbon rather than the chromite under these conditions. Dawson and Edwards[32] proposed that the mechanism of the reduction in the presence of the liquid fluoride flux was the dissolution of chromite spinel constituents in the fluoride flux, diffusion of the chromium and iron oxide ions to the reducing agent surface where reduction to metal takes place and precipitation of the magnesium and aluminium oxides as a spinel occurs.

Fukagawa and Shimoda[33] in a recent paper (1987) investigated the smelting reduction rate of mixtures of chromite, quartz and limestone (which had been sintered together in a separate prior step) in a graphite crucible. They found that undissolved chromite particles persisted in the slag until the reduction was complete and that only a very small amount of metal (mainly iron) was associated with the chromite particles. A reduction mechanism, illustrated in Fig. 2 and consisting of the following steps was proposed:

(i) dissolution of chromite ore particles into the slag, and

(ii) reduction of chromium and iron oxide in the slag at the slag graphite interface.

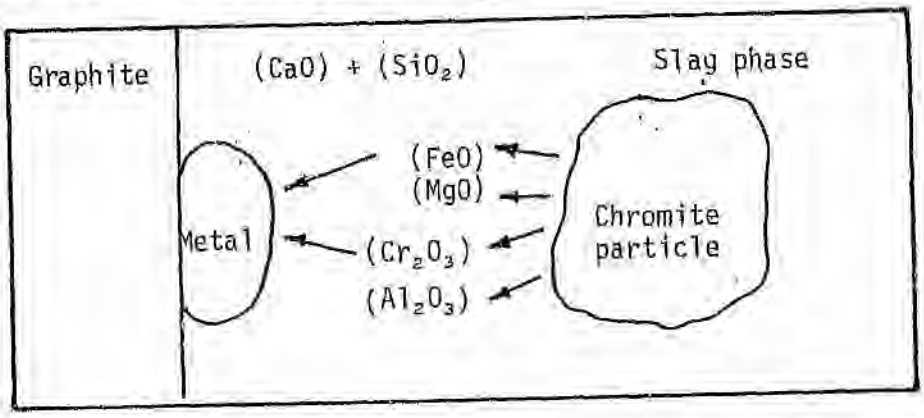


Figure 2. Smelting reduction mechanism after Fukagawa and Shimoda[33]

The rate limiting step was found to be (ii) under the conditions of this study but the authors state that it is not clear whether the rate is controlled by transport of chromium oxide in the slag or chemical reaction at the slag-graphite interface. The reaction rate was found to decrease as the reaction proceeded while the MgO and Al_2O_3 content of the slag increased. Deliberate additions of MgO to the slag dramatically lowered the reaction rate.

Robison and Pehlke[34] investigated the kinetics of reduction of chromium oxides from a steelmaking-type slag (45 per cent CaO, 35 per cent SiO_2, 10 per cent MgO and 10 per cent Al_2O_3) by a Fe-Cr-Si alloy (10 per cent chromium, 1 per cent silicon). They proposed a reduction mechanism based on the following reactions.

$$(Cr_2O_3) + Si = (SiO_2) + (CrO) + \underline{Cr} \quad ....(8)$$

$$2(CrO) + \underline{Si} = (SiO_2) + 2\underline{Cr} \quad ....(9)$$

The reduction of Cr_2O_3 (Equation 8) was found to be rate limited by diffusion of Cr^{3+} from the bulk slag to the slag metal interface. The rate of CrO reduction (Equation 9) was found, however, to be limited to the rate of an interfacial chemical reaction. This system is more appropriate to stainless steel refining as was Rankin and Biswas's work[19] than chromite smelting since it is essentially carbon-free but the Fe-Cr-C-Si alloy formed at the carbon surface in chromite smelting creates a similar slag-metal environment. It is also interesting that Robison and Pehlke[34] found that Cr^{3+} transport was rate limiting when compared with Fukagawa and Shimoda's[33] proposed mechanism of either Cr^{3+} transport or reaction at the graphite interface.

2.4 Chromite dissolution

The role of chromite dissolution in the reduction mechanism proposed by Fukagawa and Shimoda[33] is that of an essential (but not rate-limiting) step. It is significant that complete dissolution of the chromite took place under the conditions of their study, i.e. all the chromite constituents dissolved in the slag. The chromite dissolution process that is of importance is therefore that of the original unaltered chromite and not that of a partly reduced chromite, i.e. lowered in chromium and iron oxides but enriched in magnesium and aluminium oxides. An examination of the various concentration gradients likely to be present in the smelting reduction mechanism proposed by Fukagawa and Shimoda[33] was carried out to define the dissolution process more exactly. The more general case of a Fe-Cr-C-Si alloy as the site of

reduction was used rather than graphite to account for the formation of a product layer of metal around the carbon reductant. This allows for concentration gradients of carbon in the metal phase to be set up and for the formation of chromous oxide via the equation

$$(Cr_2O_3) + \underline{Cr} = 3(CrO) \qquad \ldots.(10)$$

at the slag-metal interface. The reducing conditions will be defined by the carbon content of the alloy at the slag-metal interface, and at carbon saturation as shown earlier (see Table 2) the equilibrium activities of both Cr_2O_3 and CrO would be extremely low. The system considered is shown in Figure 3 for Cr^{3+} concentration profiles. It was assumed that the Cr_2O_3 concentration in the slag at the slag-chromite interface was in equilibrium with the Cr_2O_3 concentration in the chromite spinel at the same interface. The Cr_2O_3 concentration in the slag at the slag-metal interface was similarly assumed to be in chemical equilibrium with the carbon dissolved in the metal, as defined in Equation (2). The steps associated with the reduction of Cr_2O_3 from the spinel to metal at the slag-metal interface in the general case were considered to comprise the following:

(i) solid-state diffusion of Cr^{3+} ions to the chromite-slag interface,

(ii) dissolution of Cr_2O_3 into the slag at the interface at a rate sufficient to maintain the equilibrium Cr_2O_3 concentration in the slag,

(iii) liquid-state diffusion of Cr_2O_3 through the static boundary layer around the chromite particle,

(iv) transport of the Cr_2O_3 through the bulk slag to the slag-metal boundary layer, which may take place by bulk movement of the slag in well-mixed systems or by diffusion through the slag in static systems,

(v) diffusion of the Cr_2O_3 through the static boundary layer surrounding the slag-metal interface, and

(vi) reaction of Cr_2O_3 at the interface at such a rate as to maintain the equilibrium concentration of Cr_2O_3.

Figure 3: Possible concentration gradients of Cr_2O_3 in a chromite-slag-metal-carbon system

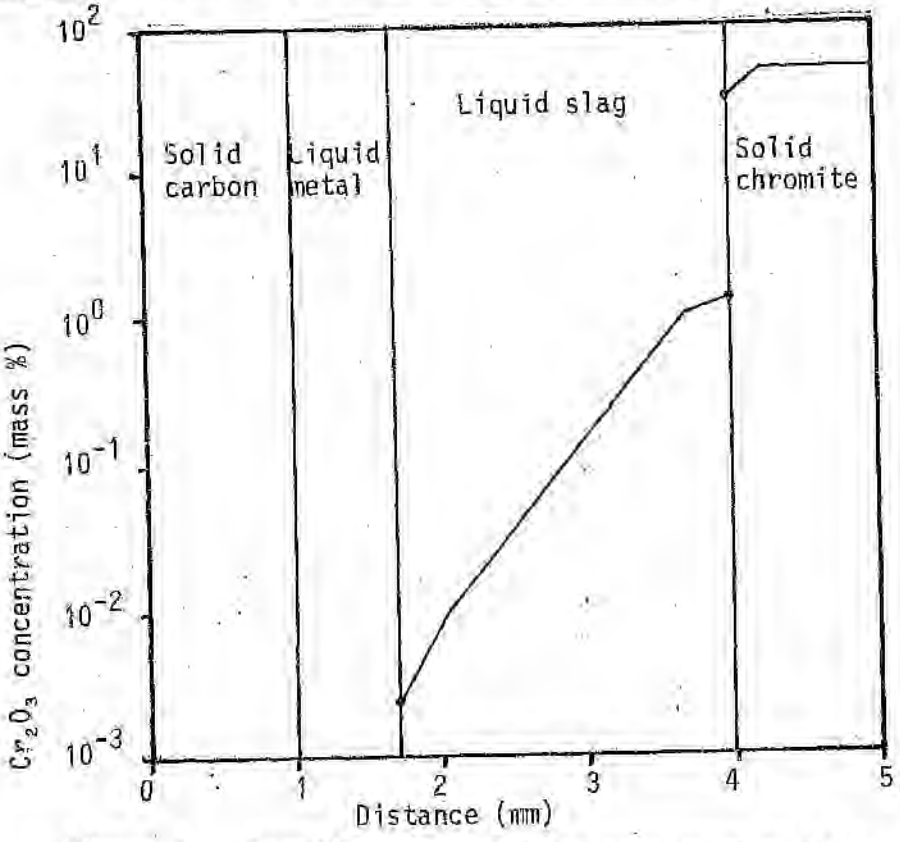


Figure 3. Possible concentration gradients of Cr_2O_3 in a chromite-slag-metal-carbon system

The governing parameter for the dissolution process is the equilibrium concentration of Cr_2O_3 in the slag at the chromite-slag interface, which is also the saturation concentration of Cr_2O_3 or the maximum solubility. This parameter will depend on the temperature, the slag composition and the chromite composition. The saturation concentration of Cr_2O_3 defines the maximum concentration gradient which can form in the slag phase and therefore affects the driving force for all the subsequent diffusional transport steps. The saturation concentration of Cr_2O_3 in air in the MgO-SiO_2-Cr_2O_3 system is less than 5 per cent[11] and therefore the transport of Cr_2O_3 in such slags may well be slow.

The solubilities (saturation concentrations) of all the spinel constituents are of significance in the complete dissolution of chromite. However, because the solubilities of MgO, Al_2O_3 and FeO are much higher (typically > 10 per cent) in similar

slag systems[11] they are less likely to become rate limiting steps. Fukagawa and Shimoda[33] found that complete dissolution took place in their slag system but that the increasing levels of MgO and Al_2O_3 in the slag (from the dissolved spinel) as the reduction proceeded slowed the reaction rate considerably. The concentrations of MgO and Al_2O_3 attained in a steady-state operation will depend upon the nature and quantity of fluxes added and it can be envisaged that these concentrations could exceed the saturation concentrations defined by the original chromite composition. The MgO and/or Al_2O_3 in the chromite spinel will not therefore dissolve into such a slag and the Cr_2O_3 and FeO will consequently have to diffuse through the solid spinel structure to dissolve in the slag. The much lower diffusivities of ions in solid solutions compared with liquid solutions[35] could well result in the chromite dissolution step becoming rate limiting. The importance therefore of determining the saturation concentrations of all the chromite spinel constituents, but particularly the values for MgO and Al_2O_3, to determine the optimum flux additions becomes evident.

3 EXPERIMENTAL PLANNING

The planning of the final experimental work was aided considerably by preliminary testwork to demonstrate the feasibility of some of the experimental procedures. These preliminary tests will not be reported here as they were not central to the objective of the investigation.

3.1 Objectives and Scope

The primary objective of the experimental testwork was the determination of the saturation concentrations of the spinel constituents of a Transvaal chromite in silicate slags at smelting temperatures (1650°C). It was decided to restrict the scope of the investigation to the effects of slag composition and temperature while keeping the remaining major variable, the chromite composition, constant. An inert atmosphere was therefore necessary to avoid altering the

composition of the chromite by either oxidation or reduction. The choice of a fixed chromite composition rather than a fixed slag composition was made because of the wide range of compositions that could be investigated by a simple choice of fluxes, compared with the rather narrow compositional ranges of natural Transvaal chromites which were readily available[27]. The preparation of synthetic chromites or the use of chromites from other countries was not considered for this study, but would provide a wider range of chromite compositions, e.g. Fe^{2+}/Fe^{3+} ratio, Cr/Fe ratio and MgO/Al_2O_3 ratio.

It was further decided to consider only slag constituents which were currently being employed in the chromite smelting industry, i.e. $CaO-SiO_2-MgO-Al_2O_3$ slags, although the work of Dawson and Edwards[32] had shown the beneficial effects of calcium and sodium fluorides on the dissolution process at 1300°C. Commercial grades of fluxing agents, e.g. limestone and quartz rather than chemically pure materials were used, again to simulate actual industrial practice as closely as possible. The choice of a $CaO-SiO_2-MgO-Al_2O_3$ slag system implied that only the CaO/SiO_2 ratio need be considered in the selection of the slag compositions to be investigated since the MgO and Al_2O_3 concentrations would be fixed by the chromite composition at equilibrium. The qualitative behaviour of the slag-chromite interaction under non-equilibrium conditions is, however, also of interest in understanding the dissolution process. Slags were therefore chosen with a range of MgO and Al_2O_3 contents as well as CaO/SiO_2 ratios so that the approach to equilibrium could be varied. The selection of the slag compositions also defined the maximum range of temperatures that could be investigated such that the temperature of any experiment was always above the liquidus temperature of the slag being used.

3.2 Prior Work

The dissolution of a cube of chromite into a liquid slag , in a molybdenum crucible, was studied by Urquhart[31] at temperatures from 1500°C to 1620°C by measuring the concentrations of iron and chromium in the slag after tests

lasting from 0,25 to 4,0 hours. A slag containing 21,4 per cent MgO, 18,6 per cent Al_2O_3 and 50 per cent SiO_2 was used for all the tests. It was found that the dissolution of pure unreacted chromite at 1500°C was 'exceedingly slow', and therefore all the dissolution experiments used a slightly pre-reduced chromite (i.e. 6,6 per cent of the iron and 0,6 per cent of the chromium). The initial extent of dissolution was found to be a linear function of the square root of time in accordance with Fick's law of diffusion. The dissolution rate decreased later however, which was attributed to the approach of the chromium and iron contents of the bulk slag to the saturation concentrations. The data of Urquhart[31] was used to estimate the likely values of the saturation concentrations of iron and chromium at 1580°C, expressed as FeO and Cr_2O_3, as ~3,5 per cent and ~3,1 per cent respectively. These values are difficult to relate to a single definite chromite composition because of the slight pre-reduction of the chromite.

Roos[36] investigated the dissolution of a rotating cylinder of a Transvaal chromite from the LG-6 layer of the Bushveld Complex, into a slag contained in a molybdenum crucible, under an inert gas atmosphere. A temperature range of 1550°C to 1700°C was used for time periods of between 1 and 3 hours. The initial slag composition was the same in all tests (0,35 per cent FeO, 45,3 per cent SiO_2, 29,2 per cent MgO, 18,0 per cent Al_2O_3 and 8,5 per cent CaO). Very limited dissolution was found to take place over the ranges of the experimental variables of time and temperature. Maximum values of 0,9 per cent FeO and <1,0 per cent Cr_2O_3 were measured in the slag. A 'reaction-rim', some 30 μm thick, was found to have formed at the slag-chromite interface which differed substantially in composition from the original chromite (see Table 4). The 'reaction-rim' had been denuded of chromium and iron, enriched in magnesia and alumina and was stable under stirred conditions with respect to the surrounding slag. Since both Urquhart[31] and Roos[36] used slags that were similar in composition to the final slags from submerged-arc furnaces and did not observe any significant dissolution of unreduced

chromite the possibility that slag composition controls the dissolution rate should be considered. The loss of undissolved chromite industrially may, therefore, be a consequence of the introduction of largely unreduced chromite into a slag of final composition, i.e. rich in MgO and Al_2O_3 rather than incipient slag consisting largely of SiO_2 and CaO.

Table 4: Effect of dissolution on chromite composition after Roos[36] (mass %)

	Cr_2O_3	FeO	SiO_2	MgO	Al_2O_3	CaO
Chromite	48,2	24,7	0,03	11,3	13,6	0,01
Chromite-rim	32,0	1,7	0,24	23,7	38,0	0,06

The role of reducing conditions in the dissolution process is undoubtedly important as shown by Urquhart[31] and in the work of Dawson and Edwards[32] where they found that 'spinel dissolves only when it is in close proximity to a reductant particle' and suggested that this may be a result of the 'melt immediately adjacent to the chromite particle becoming saturated in one component, probably Cr_2O_3'.

3.3 Design of Experiments

The experimental testwork was required to provide conditions where silicate slags with a range of CaO/SiO_2 contents could come into chemical equilibrium with a natural chromite of original and unaltered composition. The requirements of chemical equilibrium and unaltered composition immediately necessitated the use of an isothermal system under an inert atmosphere. The system can be considered therefore, as a condensed, isothermal, seven component system, i.e. Cr_2O_3,

Al_2O_3, Fe_2O_3, MgO, FeO, SiO_2 and CaO. There are two phases present throughout, solid chromite spinel (Cr_2O_3, Fe_2O_3, Al_2O_3, MgO, FeO) and liquid slag containing all seven components. An inert (argon) atmosphere was used thereby fixing the oxygen partial pressure in the system by the FeO/Fe_2O_3 ratio present in the original chromite spinel provided that no gain or loss of mass took place. The actual oxygen partial pressure cannot, however, be determined since the activities of the FeO and Fe_2O_3 in either the solid spinel or the liquid slag are unknown. The chromite spinel can be regarded[13] as a complete solid solution above 1000°C of the various components with essentially insignificant solubility for SiO_2 and CaO based on cation size. The chromite phase was assumed to display complete stoichiometry with regard to divalent and trivalent cations, i.e. 1:2 molar ratio although a small degree of cation deficiency in natural chromites has been reported[13]. Therefore, the solid phase can be completely defined by fixing two of the trivalent cation concentrations, one of the divalent cation concentrations and assuming complete spinel stoichiometry exists. The phase rule indicates that for an isothermal, condensed system of two phases and seven components that the system has five degrees of freedom. The remaining independent variable is therefore either the CaO or SiO_2 content of the slag, since at equilibrium the solid phase spinel composition will fix the compositions of the corresponding five liquid phase components. An excess of a natural chromite spinel as the solid phase will result in an effectively constant solid phase composition fixing four of the available degrees of freedom. The selection of a fixed

$CaO:SiO_2$ ratio then defines the system completely and the effect of this ratio upon the slag composition in equilibrium with a standard, known natural chromite can therefore be determined.

Since the solid phase composition is constant the activities of each of the five component species are also constant at any given temperature. The equilibrium condition between the solid and liquid phases requires therefore that the activities of Cr_2O_3, FeO, Al_2O_3, MgO and Fe_2O_3 in the liquid slag phase are also constant. The independent variations of the $CaO:SiO_2$ ratio in the slag phase in equilibrium with a constant solid chromite phase effectively determines the corresponding variation of the activity coefficients of Cr_2O_3, Al_2O_3, MgO, FeO and Fe_2O_3 in the slag phase.

The need to investigate a wide range of slag compositions in the $MgO-Al_2O_3-SiO_2-CaO$ system with significant solubility for the refractory spinel forming oxides MgO and Al_2O_3 imposed severe constraints on the use of conventional oxide crucibles. It was also desirable to maintain an excess of chromite over slag to maintain a constant chromite composition. These two considerations led to a decision to investigate the use of chromite crucibles. Two advantages were identified over the alternative possibility of using an inert metal crucible, e.g. platinum. Firstly a simple system consisting only of the materials to be brought into equilibrium and secondly the practical possibility of sectioning each crucible and its contents for subsequent microscopic investigation. The major disadvantage was the need to develop a technique to

manufacture chromite crucibles of suitable dimensions and quality (e.g. resistance to thermal shock, low and high temperature strength, etc.).

Preliminary tests on chromite crucibles, during the development of a suitable manufacturing technique, revealed that crucibles with a high (~30 per cent) porosity provided good conditions for the equilibrium of the slag and chromite phases within the porous walls of the crucible. The slag was found to alter in composition as it flowed through the pores of the crucible wall by successive contact with the chromite grains, until in the outer portions of the chromite wall no further changes were observed. It was considered that the slag and chromite in these outer areas were in chemical equilibrium.

It was decided to use this method of attaining equilibrium in the experimental programme because of the following advantages:

(i) independent of the starting slag composition, particularly MgO and Al_2O_3,

(ii) provides a record of the approach to equilibrium through the crucible wall, and

(iii) avoids repetitive experiments with slightly different slag compositions to 'home-in' on the equilibrium composition.

The major disadvantage of this method is the need for micro-analytical techniques (energy dispersive spectroscopy) to determine the slag composition and therefore it is not

possible to determine the oxidation states of the elements present. This is of particular significance for the measurement of the Fe^{2+}/Fe^{3+} ratio in the slag or chromite phases.

4 EXPERIMENTAL WORK

The final experimental programme was decided upon based on the preliminary experiments to establish the technique required and the feasibility of the measurements. A description of these methods is given here in the following sub-section.

4.1 Preparation of Materials

The preparation of the two materials required for the testwork, chromite crucibles and the master slags are described separately for clarity.

4.1.1 Chromite crucibles

A 300 kg sample of chromite from the LG-6 layer of the Bushveld Complex[37] was obtained from the Winterveld Mine as a standard source for the entire investigation. Approximately 200 kg was lightly ground and then tabled by the Ore Dressing Division of Mintek to produce several low-gangue content fractions. The masses and chemical analyses of these fractions are shown in Table 5.

Table 5: Winterveld chromite fractions after gangue removal

Fraction	Mass kg	Chemical analysis (mass%)								
		Cr_2O_3	FeO$^{\gamma}$	SiO_2	CaO	MgO	Al_2O_3	TiO_2	MnO	Total
C1	29,5	48,7	26,0	<0,1	0,08	10,7	13,4	0,18	0,34	99,4
C2	27,1	48,6	26,0	<0,1	0,04	10,8	13,5	0,17	0,32	99,4
C3	17,4	48,7	26,0	<0,1	0,05	10,9	13,6	0,17	0,33	99,8
M1	11,0	47,5	25,5	<0,1	0,12	10,7	13,0	0,16	0,33	97,3
M2	36,6	46,8	25,6	<0,1	0,06	10,8	12,8	0,17	0,32	96,6
-	-	(47,7	25,8	<0,1	0,06	10,9	13,5	0,17	0,33	98,4)*

γ. Total iron expressed as FeO

* Duplicate analysis on fraction M2

It was decided to consolidate the fractions C1, C2 and C3 as the standard chromite source for the preparation of the chromite crucibles.

It was originally decided to produce chromite crucibles large enough for the contained liquid slag to be stirred in future experiments. This relatively large size (58 mm high and 36 mm in diameter) and length:diameter ratio made the use of dies and hydraulic pressing problematical. A technique consisting of wet-binder additions, hand-ramming, drying and sintering under argon was adopted. The choice of a binder was restricted to elements already present in the experimental

system (i.e. chromium, iron, silicon, magnesium, calcium, aluminium, oxygen) and an aqueous solution of CrO_3 was selected. The variables considered and the ranges investigated in the development of a practical technique for the manufacture of these crucibles were:

(i) chromite particle size distribution, 40 per cent <150 μm to 73 per cent <150 μm,

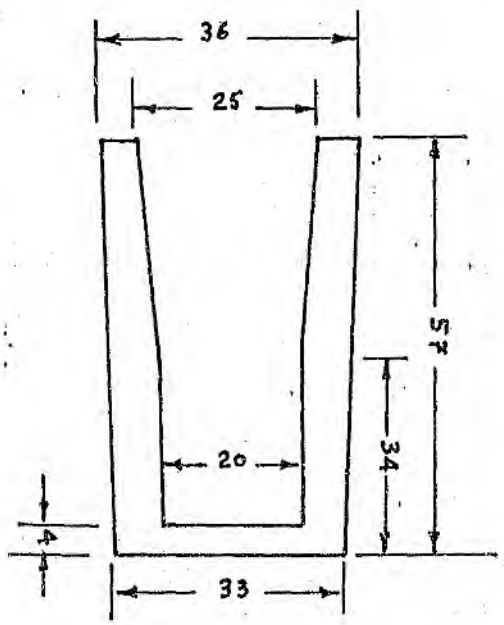
(ii) CrO_3 solution concentration, 5,0 to 11,5 per cent m/v,

(iii) liquid:solids addition for binder addition, 8 to 11 per cent v/m,

(iv) mould material, mild steel, stainless steel, teflon, and

(v) sintering temperature, 1400°C to 1550°C.

The final technique produced crucibles with the typical dimensions shown in Figure 4 with a success rate of greater than 90 per cent. The values of the various parameters used in the successful technique are given in Table 6. The crucibles had an average porosity of 38,1 per cent determined by the evacuation method[38] and an average bulk density of 2,76 g cm^{-3}. No significant change in chemical composition could be observed as a result of the procedure adopted for the crucible preparation (see Table 7). The details of the particle size distribution of the chromite which was used for the preparation of the crucibles is shown in Table 8.



Dimensions	:	mm
Tolerance	:	$\pm$ 1 mm
Average mass	:	92,52 $\pm$ 1,55 g
Average porosity	:	38,1%
Average bulk density	:	2,76 g cm^{-3}

Figure 4. Chromite crucible

Table 6: Parameters used in the preparation of chromite crucibles

Parameter	Value
Chromite particle size*	73% <150 μm, 17% <75 μm
CrO_3 binder solution concentrate	11% m/v
Liquid binder addition	9% v/m
Outer mould	Teflon
Inner mould or former	Polished stainless steel
Drying oven temperature	90°C
Drying oven time	16 h
Sintering temperature**	1550 ± 10°C
Sintering atmosphere	Spectrographic grade argon

Notes:

* The entire 20 kg stock of purified chromite was milled in a ball mill with alumina balls to reach a particular size distribution similar to the preliminary test samples. This ensured that all crucibles made subsequently used a constant size distribution material.

** A vertical-tube molybdenum wire resistance furnace, to be described in a later section, was used. The work tube was well sealed and purged with spectrographic grade argon to maintain an inert sintering atmosphere.

Table 7: Composition of chromite and a sintered chromite crucible

Material	Chemical composition (mass%)									
	Cr_2O_3	FeO	Fe_2O_3	MgO	Al_2O_3	SiO_2	CaO	TiO_2	MgO	Total
Chromite	47,5	18,5	7,5	9,8	13,1	<0,3	<0,2	0,6	0,3	97,8
Sintered chromite crucible	47,9	18,2	7,6	9,8	12,9	<0,3	<0,2	0,5	0,3	97,7

Table 8: Particle size distribution of the chromite

Particle size range µm		Distribution mass %	Cumulative distribution mass %
	>150	27,1	27,1
<150,	>125	15,3	42,4
<125,	>106	17,1	59.5
<106,	> 90	21,3	80,8
< 90,	> 75	1,9	82,7
< 75,	> 63	14,5	97,2
< 63,	> 53	0,6	97,8
< 53,	> 45	0,4	98,2
< 45,	> 38	0,4	98,6
< 38		0,4	100,0

4.1.2 Master slags

A d.c. transferred plasma arc furnace was selected to prepare the slags because of the large volumes of slag that could be produced and the ease of melting non-metallic materials which this facility offers. The 100 kVA plasma facility in Bay J at Mintek was fitted with a graphite crucible (see Figure 5) and the four raw materials were charged to the feed hoppers. These materials were industrial grades of quartz, limestone, burnt magnesite and alumina, in order to simulate an industrial slag formed from standard fluxes as far as possible. The plasma arc was struck on the bottom of the crucible and the feed was started at low rates (~2 kg/h) immediately. This was increased to ~15 kg/h as the molten pool was observed to increase in diameter. The feed-rate of each material was independently controlled to supply the correct mixture of material to the furnace throughout the melting process. A total of between 4,6 kg and 9,7 kg was fed to each heat. The furnace was operated at between 60 V, 500 A and 75 V, 600 A aiming to maintain a stable arc column and avoid overheating the roof. A series of eight heats were carried out, each of which was poured into mild steel tapping trays, cooled and broken out. The masses of each component fed to the furnace are shown in Table 9. The solidified slag was crushed to 100 per cent < 0,5 mm and hand-sorted to remove any metallic prills present. These resulted from the reduction of the iron oxide impurities present in the raw materials by the graphite crucible and typically less than 20 g of prills were removed. The material was then roasted in

large open trays at 550°C for approximately 16 hours, to oxidize any small metallic iron or carbon particles. The roasted slags were then milled, sampled for chemical analysis and stored in sealed containers. The chemical analyses of the slags prepared in this way are shown in Table 10. The CaO/SiO_2 ratio ranged from 0,04 to 0,65 while the MgO contents fell between 4,5 and 29,4 mass per cent and the Al_2O_3 contents varied between 0,9 and 28,8 mass per cent. The compositions of the slags may be represented on a pseudo-tenery diagram (see Fig. 6) as $(SiO_2 + CaO) - MgO - Al_2O_3$. This form of representation was chosen to show the relative contents of MgO and Al_2O_3, as spinel forming oxides, as well as the total content of fluxing components $(SiO_2 + CaO)$, as non-spinel forming oxides.

Table 9: Preparation of master slags

Slag no.	Mass of raw material added (kg)			
	Quartz	Limestone	Magnesite	Alumina
1A	4,14	4,32	1,15	-
1B	4,17	4,45	1,15	-
2	6,61	4,84	1,22	1,80
3	4,17	-	1,56	1,94
4	2,65	0,42	1,89	2,25
5	3,36	-	1,89	2,24
6	4,03	-	2,66	0,75
7	4,03	5,70	-	-

Note: (1) Quartz and limestone from G & W Base Minerals
(2) Magnesite (dead burnt) from Vereeniging Refractories
(3) Alumina (Bayer 99% Al_2O_3) from Alusaf

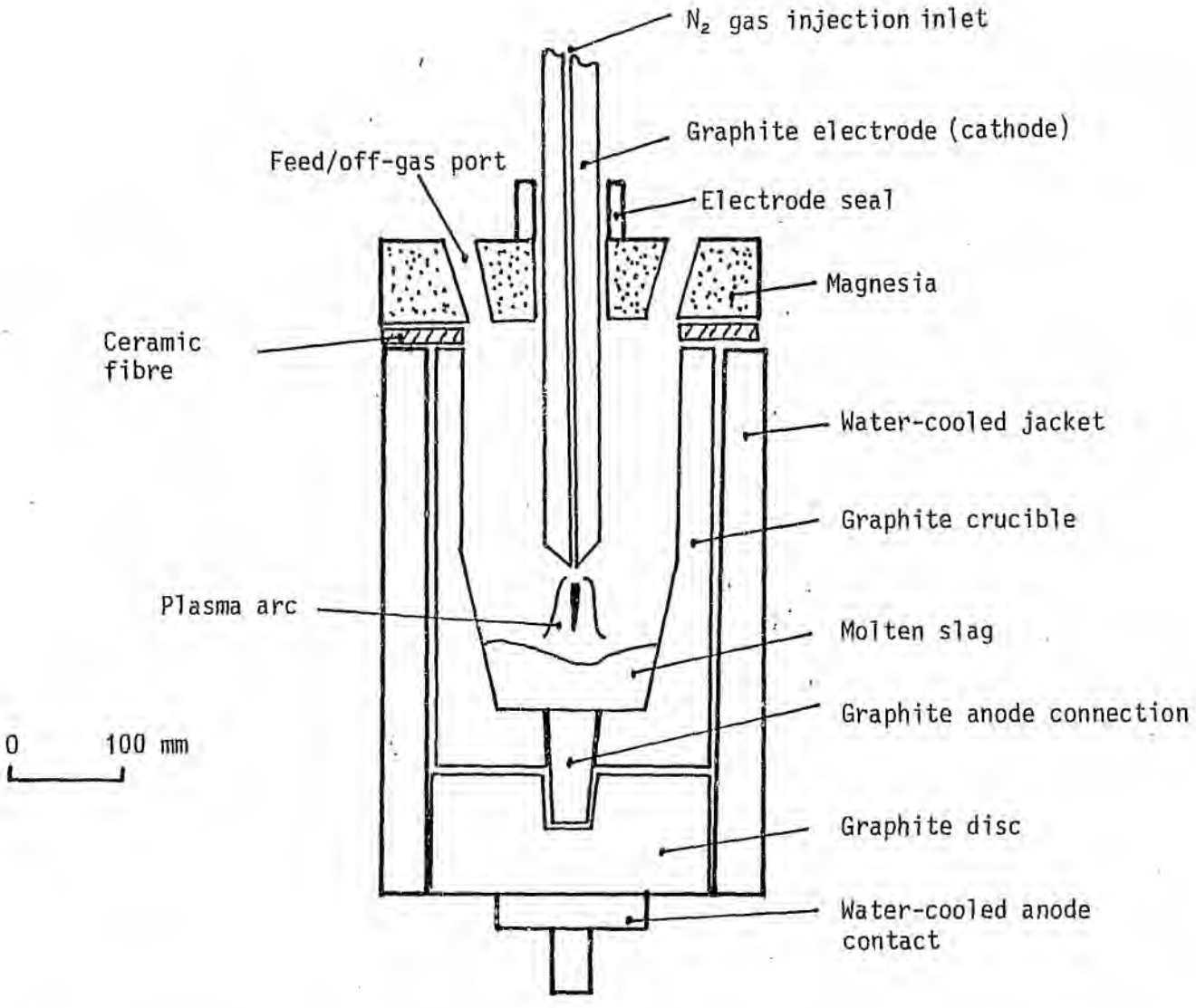


Figure 5. 100 kVA graphite crucible plasma furnace

TABLE 10

CHEMICAL ANALYSES OF MASTER SLAGS

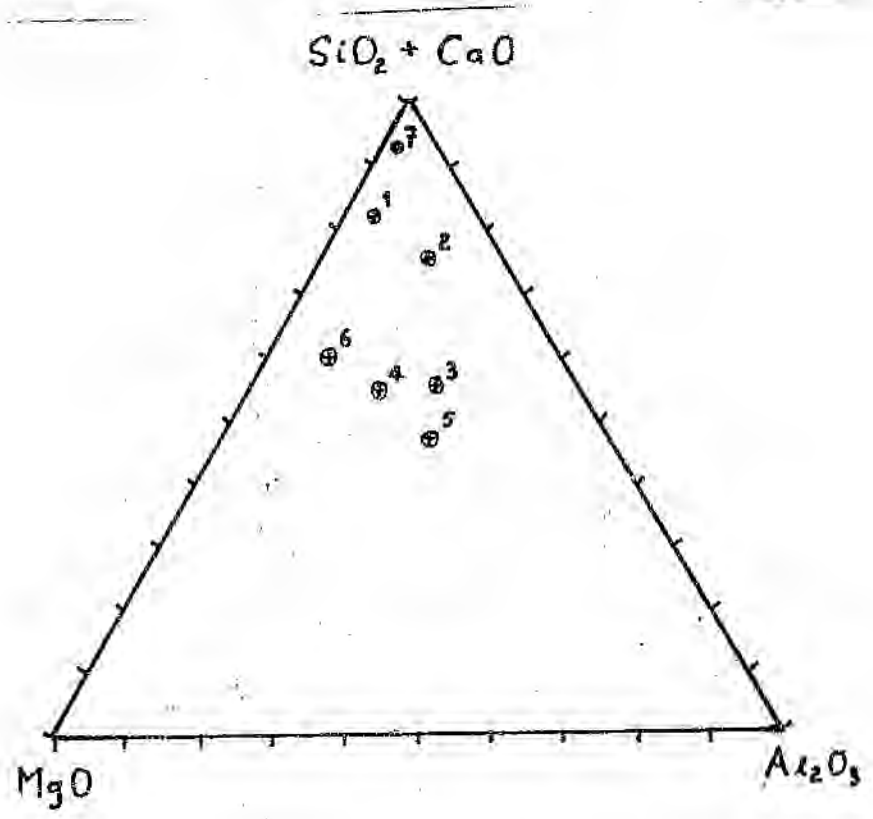
Slag no.	Composition (mass %)									
	SiO_2	CaO	MgO	Al_2O_3	Cr_2O_3	FeO	Fe_2O_3	Na_2O	K_2O	CaO/SiO_2 Mass ratio
1A	53,5	25,6	13,0	4,0	0,02	0,5	0,1	0,03	0,05	0,48
1B	53,8	27,7	14,6	0,9	0,02	1,3	0,1	0,13	0,06	0,52
2	52,0	20,6	9,8	14,4	0,02	1,0	0,1	0,02	0,04	0,40
3	52,7	2,0	18,2	24,3	0,10	0,3	0,2	0,16	0,02	0,04
4	42,2	11,4	26,8	18,0	0,22	0,3	0,1	0,12	0,04	0,27
5	44,3	1,1	23,1	28,8	0,02	0,8	<0,1	0,09	0,05	0,03
6	55,1	4,0	29,4	8,9	0,02	0,5	0,1	0,04	0,07	0,07
7	55,0	35,9	4,5	1,4	0,09	0,8	0,1	0,05	0,04	0,65

Notes: (i) MnO <0,15 per cent)
TiO_2 <0,20 per cent) For all slags
ZnO <0,003 per cent)

(ii) Fe_2O_3 calculated from total iron analysis less FeO contribution

(iii) Analyses by X-ray fluorescence spectrometry except Cr_2O_3 and FeO - wet chemical, Na_2O and K_2O - atomic absorption spectrometry

Figure 6: Composition of the master slags as the pseudeo-ternary (SiO_2 + CaO)-MgO-Al_2O_3



4.2 Description of Apparatus

A vertical tube furnace was used for the slag-chromite experiments to maintain an inert atmosphere and isothermal conditions. The furnace is shown schematically in Fig. 7 and is described in more detail in Appendix 2. The work tube was sealed and purged (0,21 g/min) with spectrographic grade argon (<0,002 volume per cent total impurities). The crucible was positioned on a pedestal which was connected to a rack and pinion mechanism to position the crucible accurately in the furnace hot zone and to allow rapid removal of the sample after the conclusion of the experiment. A rubber bellows provided a gas-tight seal on the work-tube while allowing free

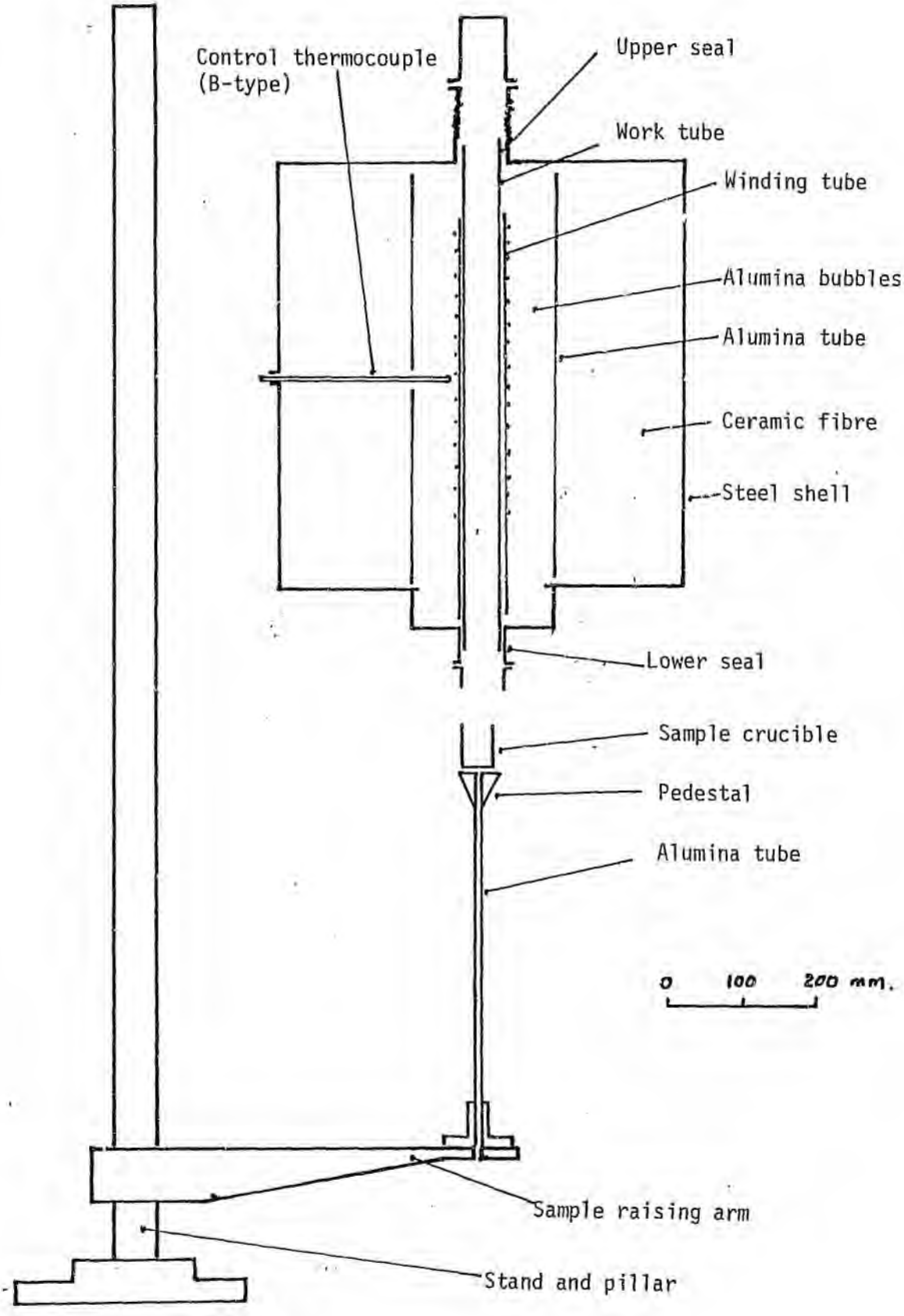


Figure 7. Schematic arrangement of vertical tube furnace

movement of the pedestal and crucible. The furnace was heated by a molybdenum wire element wound onto a recrystallized alumina tube fitted close to the work tube (clearance ~ 2 mm). Alumina bubbles formed the primary insulation layer followed by a ceramic fibre blanket. The heating element was enclosed in a sealed steel shell through which a stream (0,17 g/min) of spectrographic grade argon flowed to prevent oxidation of the molybdenum wire. The winding spacings were varied to obtain a constant temperature hot zone (± 5°C) of 70 mm in length in which the crucible was positioned. Temperature measurements were made by a B-type thermocouple (6 per cent RhPt/30 per cent RhPt) 10 mm above the upper edge of the crucible. The power input to the heating element was supplied by a thyristor converter controlled to maintain a constant temperature adjacent to the element winding. A second B-type thermocouple, fitted horizontally through the shell, was used to provide this signal. This arrangement limited temperature variations over 15 minute periods to an average value of ± 3°C and maximum values of ± 7°C while the long term drift (over 12 hours) was typically less than 4°C.

4 3 Experimental Method

The furnace temperature in this hot zone was adjusted to the desired level (1550 or 1650°C) and allowed to stabilize for twenty-four hours with an empty chromite crucible in the hot zone. The temperature at three different positions (see Fig. 8) within the crucible as well as at the usual measuring position was then determined. Finally, a specially calibrated (see Appendix 3) reference thermocouple was used to check the

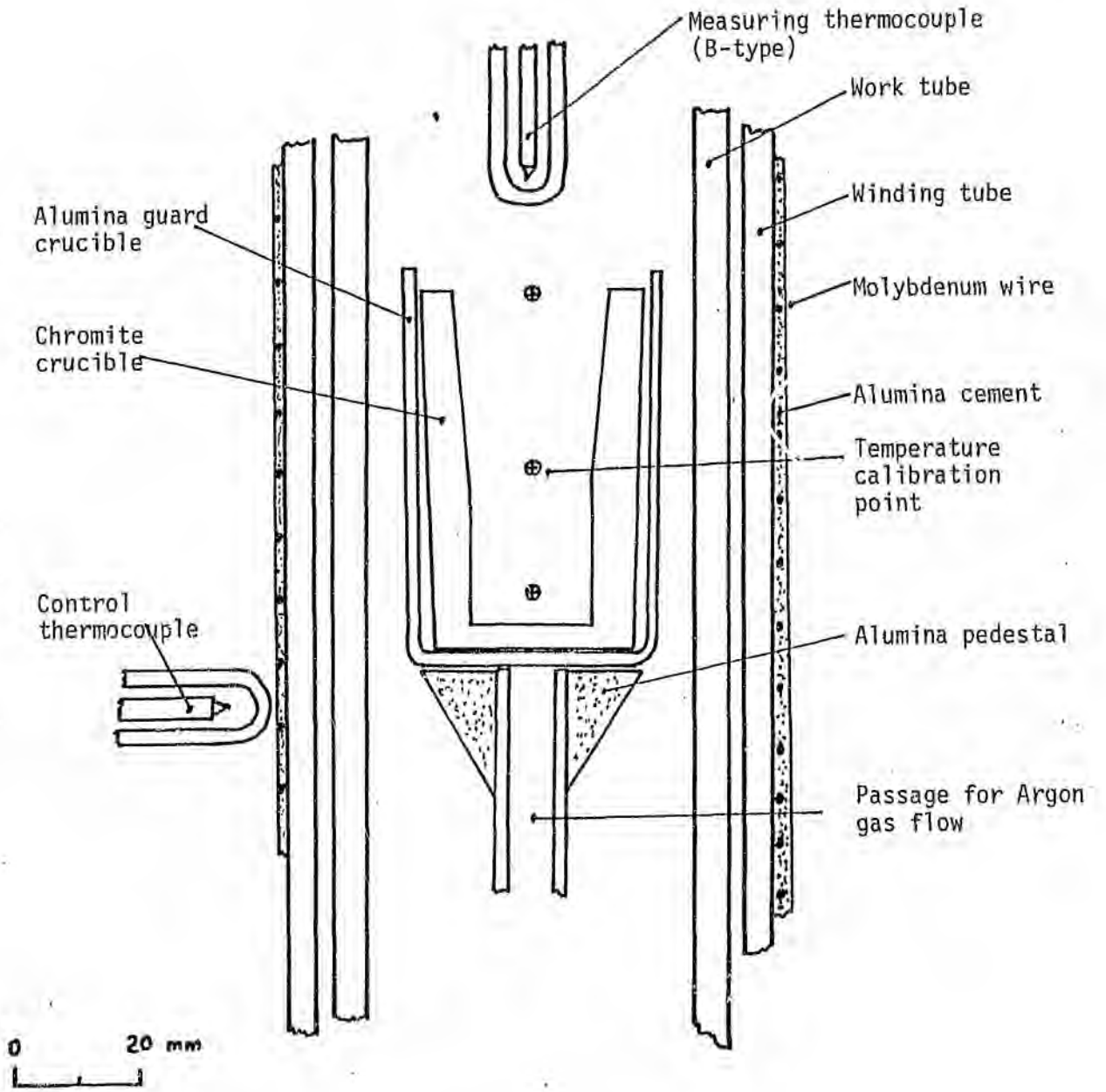


Figure 8. Arrangement of crucible and thermocouple

accuracy of the measuring thermocouple. All temperature measurements were made using a FLUKE digital thermometer (Model 2166A). The FLUKE thermometer was checked by using a galvanometer (accurate to 0,01 mV) and no discrepancy greater than 1°C was observed.

Once a well-determined hot zone temperature had been established a series of tests in which chromite crucibles were systematically contacted with the various master slags was carried out. The procedure adopted was as follows:

(i) weigh and fill a chromite crucible with one of the master slags, then reweigh,

(ii) place the chromite crucible into a recrystallized alumina guard crucible (see Fig. 8) and position on top of the furnace pedestal,

(iii) seal the bellows up around the crucible, raise into the holding position (~ 200°C) and purge with argon for 10 minutes,

(iv) raise in stages (~ 20 mm) over a 45 minute period until positioned in the hot zone (10 mm below the measuring thermocouple tip),

(v) retain in the hot zone for one hour (every sixth or seventh run was extended to at least eight hours),

(vi) lower rapidly (< 30 seconds) into the holding zone at approximately 200°C and allow to cool for 15 minutes,

(vii) disconnect bellows to break the furnace seal, remove the crucible, place in a dessicator and weigh the following day.

Details of the experimental runs carried out are given in Appendix 4 and summarized in Table 11.

The chromite crucibles were then sectioned and sent for mineralogical analyses. The Mineralogy Division at Mintek carried out analyses at selected points through the porous crucible wall into which the liquid slag phase had penetrated. The points were selected after microscopic examination of the crucible wall and accompanying slag phases. Analyses from preliminary tests had shown that only the edges of the chromite grains had been altered by contact with the slag phase. It was also observed that the extent of alteration diminished with distance from the inner surface of the chromite crucible wall. Since the composition of the slag phase in equilibrium with unaltered chromite was the objective of the investigation only chromite grains in the outer portions of the crucible were analysed. The centres and edges of typical chromite grains were analysed to detect any concentration gradients present. The slag phase adjacent to the chromite grains was also analysed (both the glassy matrix and any crystalline phase present within the glassy matrix). A typical example of the differences observed between the edges of the chromite grains located near the inner crucible wall and those near the outer part of the crucible wall is shown in Fig. 9 as well as the typical location of the points of analyses. Energy dispersive spectroscopy (EDS) was used on

TABLE 11

Summary of final test runs

Run no.	Slag no.(1)	Master slag (by mass)(1)			Temperature	Time	Δm(2)	ΔT(3)
		CaO/SiO_2	% MgO	% Al_2O_3	°C	h	%	°C
1/4	5	0,03	23,1	28,8	1546	2,3	0,15	4
2/4	4	0,27	26,0	18,0	1546	9,8	0,02	4
3/4	6	0,07	29,4	8,9	1549	1,0	0,03	6
4/4	3	0,04	18,2	24,3	1554	1,0	-0,04	6
5/4	2	0,40	9,8	14,4	1561	1,0	-0,06	7
6/4	4	0,27	26,0	18,0	1560	1,0	0,08	5
7/4	3	0,04	18,2	24,3	1554	8,1	-0,39	10
8/4	7	0,65	4,5	1,4	1555	0,9	-0,05	7
9/4	1A	0,48	13,0	4,0	1553	1,0	-0,01	10
1/5	5	0,03	23,1	28,8	1655	1,0	0,00	6
2/5	6	0,07	29,4	8,9	1651	1,0	-0,08	7
3/5	4	0,27	26,0	18,0	1651	1,0	0,07	7
4/5	3	0,04	18,2	24,3	1649	1,0	0,09	4
5/5	2	0,40	9,8	14,4	1653	1,0	0,13	6
6/5	5	0,03	23,1	28,8	1650	11,0	0,45	6
7/5	1A	0,48	13,0	4,0	1645	1,0	0,01	3
8/5	7	0,65	4,5	1,4	1654	1,0	0,15	8

Notes: (1) See Table 10 for definition of master slag numbers and compositions.

(2) $\Delta m = \frac{\text{mass in - mass out}}{\text{mass in}} \times 100\%$ (see Table A-1 for masses).

(3) ΔT = maximum temperature - minimum temperature (see Table A-1).

a scanning electron microscope (SEM) and on an electron microprobe (Probe) by the Mineralogy Division for the determination of the compositions of the material at the points requested. A blank sample consisting of a chromite crucible which had been subjected to the same procedure as described above but without the addition of a master slag was submitted for chemical analysis (by the Analytical Science Division at Mintek) for comparison with mineralogical analyses of the upper parts of the crucible wall which did not come into contact with a slag phase.

5 RESULTS

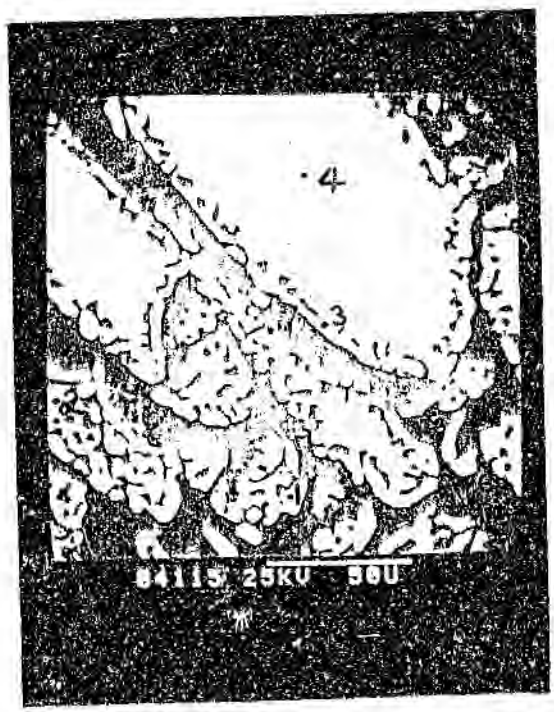
The objective of the testwork was to determine the slag composition in equilibrium with a naturally occurring chromite (from the LG-6 layer of the Bushveld Complex). This objective was sub-divided into the following steps:

(i) determine whether slag-chromite equilibrium had been attained,

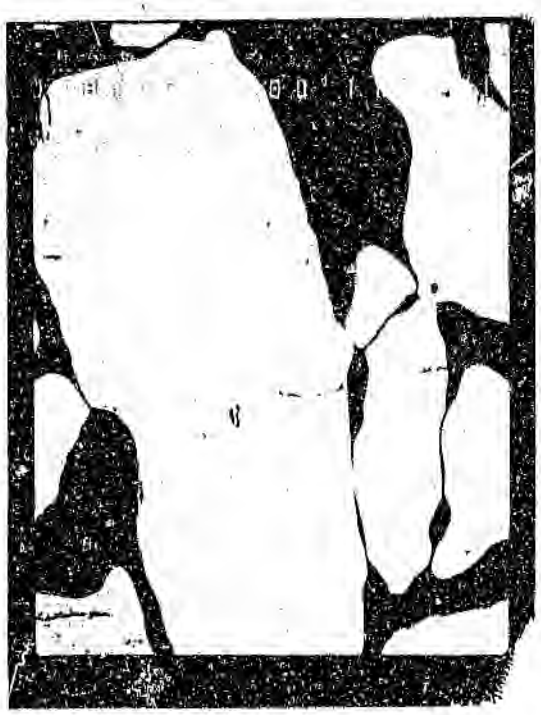
(ii) determine whether any alteration of the chromite from the original starting material had taken place, and

(iii) determine the composition of the slag in contact with the chromite.

The data was therefore analysed in stages to meet each of these sub-objectives.



Inner wall
Run no. 8/4



Outer wall
Run no. 3/4

Figure 9. Typical appearance of chromite grains near the inner and outer surfaces of the crucible wall after slag contact

The criteria selected for the attainment of equilibrium conditions was the absence of significant concentration gradients within the chromite grains. This implies that no further mass transfer between the chromite phase and the slag phase was taking place, i.e. the two phases were in chemical equilibrium. A further criteria was the absence of any significant change in the chromite composition between the tests of long duration (8 to 11 hours) compared to the short duration tests (one hour).

The micro-analyses of the centres and edges of chromite grains in the outer portion of the crucible wall which were in contact with a slag phase were carefully examined to detect any significant differences. The raw data as received from the Mineralogy Division is shown in Appendix 5 from which the means and standard deviations of the chromites' major constituents were extracted (see Table 12). The differences between the means of the Cr_2O_3, FeO, MgO and Al_2O_3 contents of chromite grains at their centres and their edges were found to be small. The differences observed (-0,57 per cent Cr_2O_3, 0,11 per cent FeO, 0,08 per cent MgO, and 0,57 per cent Al_2O_3) were not found to be significant at the 95 per cent confidence level[39].

The runs (2/4, 7/4, and 6/5) lasting longer than eight hours had average compositions that differed from the overall average composition by similarly small amounts (0,5 per cent Cr_2O_3, 0,6 per cent FeO, 0,6 per cent MgO, and 0,8 per cent Al_2O_3).

Table 12: Significance of the concentration gradients measured in chromite grains from the outer part of the crucible wall

Parameter	Species			
	Cr_2O_3	FeO	MgO	Al_2O_3
Chromite grain centres:				
Average content (mass, %)	47,20	24,57	11,75	14,77
Standard deviation (mass, %)	1,90	1,79	1,10	1,23
Number of analyses	40	40	38	40
Chromite grain edges:				
Average content (mass, %)	47,77	24,46	11,67	14,20
Standard deviation (mass, %)	2,21	1,70	1,16	1,64
Number of analyses	39	40	37	39
Pooled standard deviation (mass, %)	2,06	1,75	1,13	1,45
Standard error	0,46	0,39	0,26	0,33
Average difference, centre-edge (mass, %)	-0,57	+0,11	+0,08	+0,57
95% confidence interval	±0,90	±0,76	±0,51	±0,65

The overall average (centres and edges) composition of the chromite grains in the outer regions of the crucible wall was compared (see Table 13) with the average composition (from 10 separate analyses) of chromite grains from the upper regions of the crucible where no slag contact had taken place. Earlier chemical analysis of the blank crucible had shown that no substantial difference in composition existed between the chromite starting material and a sintered chromite crucible subjected to the conditions of these tests but without slag additions (see Table 7). The same statistical procedure as used previously[39] showed that the differences observed were not significant at the 95 per cent confidence level (see Table 13).

Table 13: Effect of slag on chromite composition at equilibrium

Description	Composition (mass, %)			
	Cr_2O_3	$(FeO)_T$	MgO	Al_2O_3
Chromite in equilibrium with slag (mean)	47,5	24,5	11,7	14,5
(Standard deviation)	2,1	1,8	1,1	1,5
Chromite not in contact with slag (mean)	48,6	25,0	12,3	13,6
(Standard deviation)	1,4	0,9	0,7	0,9
Pooled standard deviation	2,1	1,7	1,1	1,4
Standard error	0,69	0,58	0,36	0,49
Difference of means	-1,1	-0,5	-0,6	0,9
95% confidence interval	±1,4	±1,1	±0,7	±1,0

The determination of the slag composition in equilibrium with these unaltered chromite particles was based directly on the micro-analyses (see Appendix 5) of the slag phase adjacent to the chromite grains (see Fig. 9 for the typical location of the analyses points). The occurrence of a secondary crystalline phase within the slag glass matrix in many of the runs (13 out of 17 in total) complicated the determination of the overall (liquid state) slag composition. The volumetric proportions of the two phases were estimated visually by the Mineralogy Division and a correspondingly weighted average of the analyses of each of the phases was used to estimate the overall slag composition (see Table 14). Image analysis was used to check the accuracy of the visual estimate in two cases which indicated that the visual method was correct to ± 10 per cent by volume. The compositions of the two phases were generally very similar (see Appendix 5) except for the MgO content which tended to be significantly higher in the crystalline phase than the slag matrix (typically 10 to 20 per cent MgO cf. 1 to 5 per cent MgO respectively). This similarity in composition implied that the overall slag composition was not very sensitive to the weighting factor used, as well as reducing the errors associated with the assumption that the density differences between the two phases were likely to be small.

Since the chromite originally contained very little CaO and SiO_2 (< 0,2 per cent of each, see Table 7) and the final chromite grains also contain virtually no SiO_2 or CaO by virtue of their large cation size, the CaO/SiO_2 ratio should remain constant for any particular slag. This provides a useful

TABLE 14

Chromite saturated slag compositions

Run no.	Slag no.	Crystalline phase % mass	Analytical equip.	Composition (mass, %, totals normalized to 100%)							
				SiO_2	CaO	MgO	Al_2O_3	$(FeO)_T$	Cr_2O_3	TiO_2	CaO/SiO_2
1/5	5	0	Probe	51,4	1,2	11,3	17,8	16,3	1,5	1,3	0,02
2/5	6	60	Probe	49,3	3,6	13,8	14,5	15,3	1,2	1,5	0,07
2/5	6	50	SEM	50,0	4,3	12,4	14,4	16,2	0,8	1,8	0,09
3/5	4	60	Probe	46,1	15,6	6,1	15,3	14,5	1,1	1,2	0,34
4/5	3	0	SEM	52,5	1,3	15,6	14,9	13,1	1,1	1,4	0,02
5/5	2	40	SEM	47,5	14,4	6,3	17,4	12,4	1,0	1,0	0,30
6/5	5	65	SEM	52,1	1,6	15,2	14,1	14,7	1,0	1,2	0,03
6/5	5	80	SEM	52,4	1,3	14,3	12,8	16,7	1,4	1,3	0,02
7/5	1[A]	70	SEM	45,9	19,2	6,1	13,1	13,2	1,8	0,8	0,42
8/5	7	60	Probe	43,1	22,2	4,5	5,8	11,1	0,9	1,2	0,52
1/4	5	0	SEM	55,7	1,7	10,1	19,1	10,9	0,8	1,7	0,03
2/4	4	0	SEM	49,9	13,7	4,4	20,5	7,1	0,9	3,5	0,27
2/4	4	0	Probe	52,3	12,3	3,7	20,9	5,7	1,2	3,6	0,24
3/4	6	0	Probe	55,6	4,4	7,3	19,2	10,5	0,5	2,3	0,08
4/4	3	0	Probe	53,9	2,0	10,0	19,0	13,4	0,9	0,7	0,04
5/4	2	30	Probe	46,9	15,0	4,8	20,2	10,5	0,9	1,5	0,32
6/4	4	25	SEM	46,7	10,9	5,2	16,6	19,3	0,8	0,6	0,23
6/4	4	20	Probe	50,7	9,2	3,9	12,6	22,8	0,8	0,1	0,18
7/4	3	0	Probe	56,2	2,3	8,2	18,9	11,8	0,8	1,8	0,04
8/4	7	80	Probe	43,1	23,7	6,6	14,2	10,8	0,6	1,0	0,55
9/4	1[A]	80	SEM	44,9	21,0	5,8	12,5	12,4	1,1	1,0	0,47

Note: $(FeO)_T$ = Total iron expressed as FeO

means of checking on the accuracy of the overall equilibrium slag composition by comparing the CaO/SiO_2 ratio with the original master slag composition. This is shown in Fig. 10 and indicates that fairly good agreement was attained. The iron contents of the slag phase are reported as total iron expressed as FeO, although given the 7,5 per cent Fe_2O_3 content of the chromite, it is likely that a significant proportion of the iron in the slag phase was in the form of Fe_2O_3.

The effect of the CaO/SiO_2 mass ratio on the equilibrium slag composition at 1550°C and 1650°C is shown in Figs. 11 and 12 respectively. The effects of a ± 10 per cent error in the volumes of the two slag phases have been indicated by error bars and it can be seen that for the worst affected oxide, MgO, the typical error was ± 0,8 per cent MgO while the maximum error was ± 1,6 per cent MgO.

6 DISCUSSION

The results are discussed in three parts, firstly the mechanism of the porous crucible technique, its advantages and limitations. Secondly, the effects of temperature and CaO/SiO_2 ratio upon the chromite saturated slag compositions and, finally, some of the implications of these results for the smelting of chromite are considered.

6.1 The Porous Crucible Technique

The mechanism by which the slag composition changes from the initial or master slag composition to the equilibrium composition in the outer regions of the porous chromite

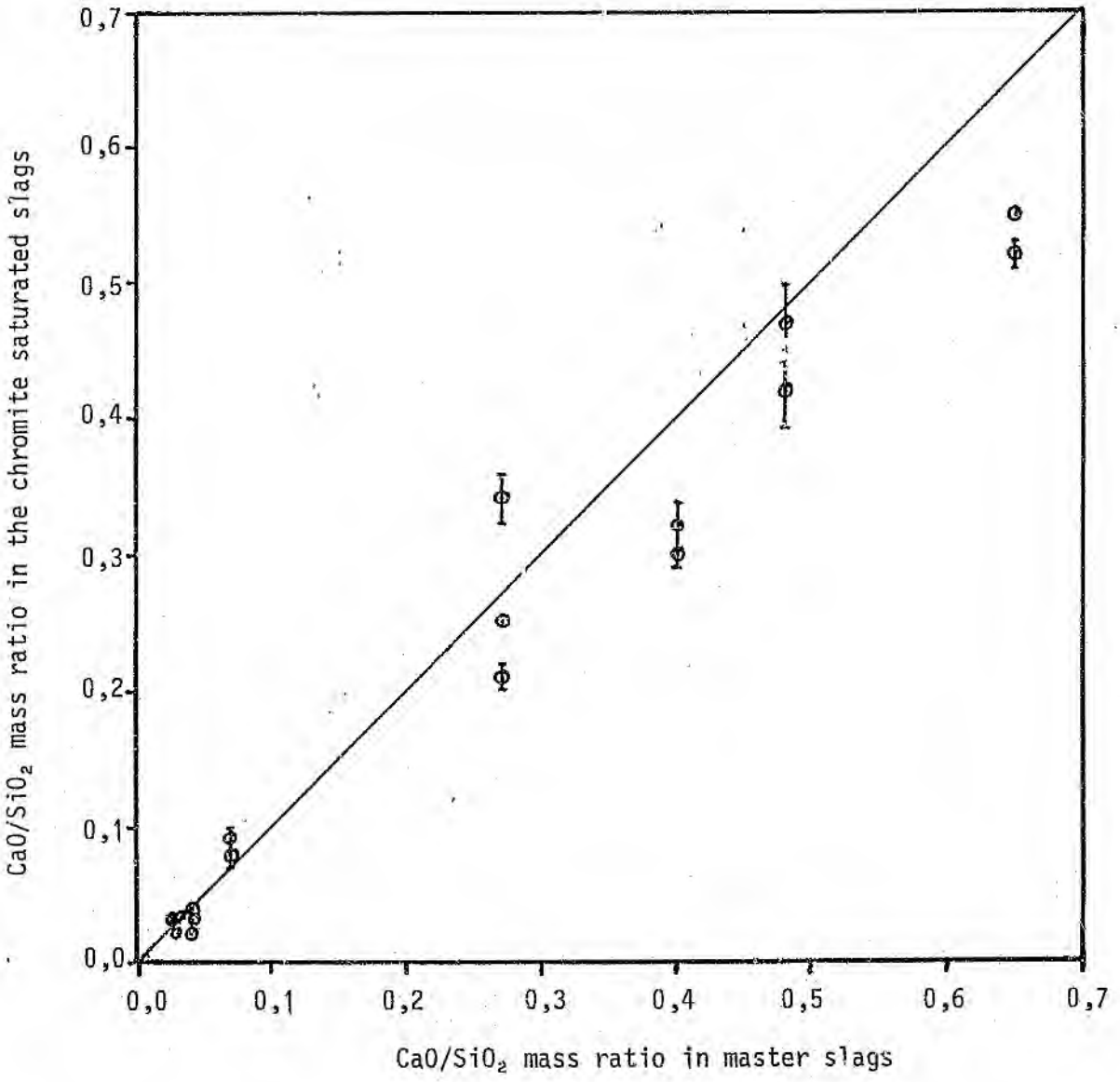


Figure 10. Comparison of the CaO/SiO_2 ratios of the master slag and equilibrium slags

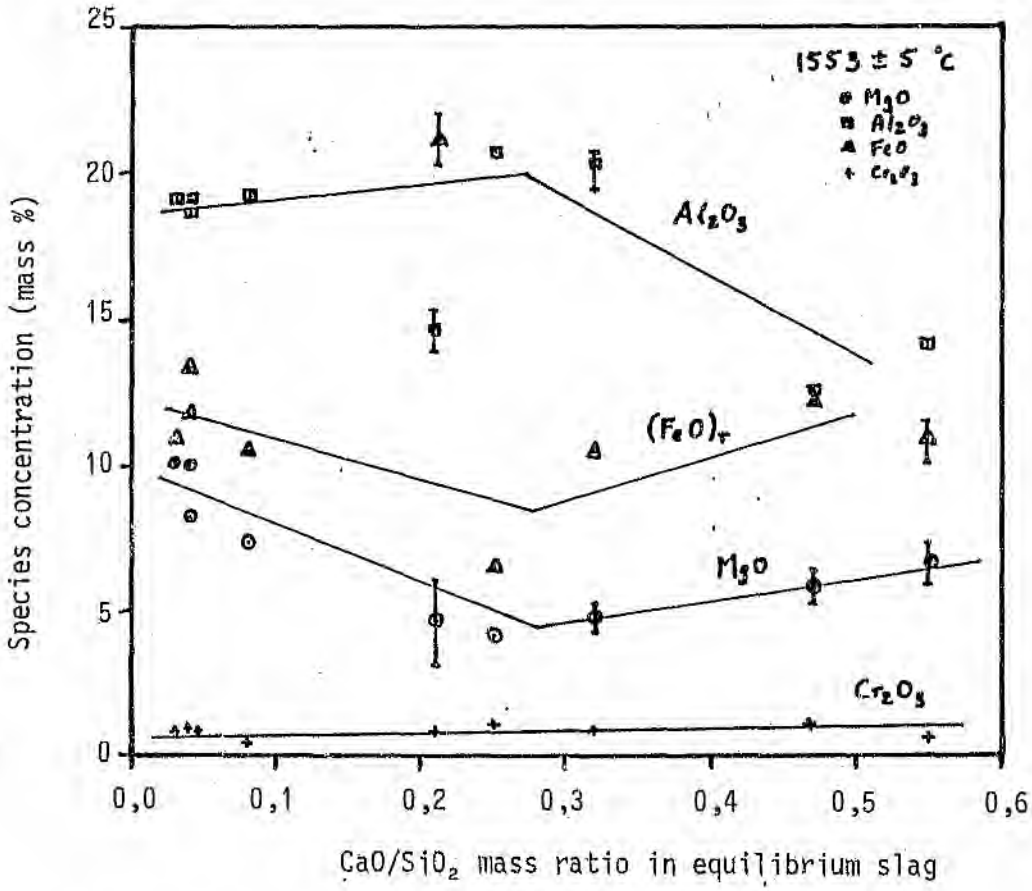


Figure 11. Composition of slags in equilibrium with chromite at 1550°C

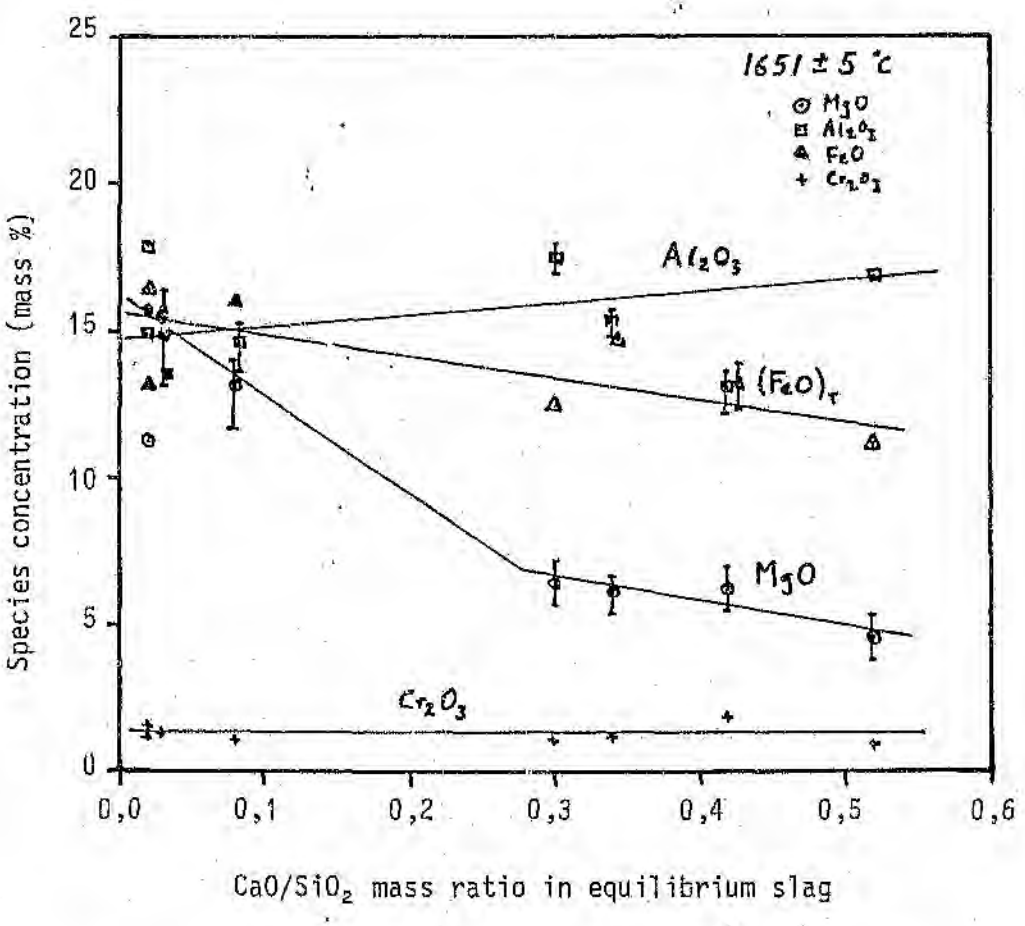


Figure 12. Composition of slags in equilibrium with chromite at 1650°C

crucible wall probably involves an exchange of chemical species with the chromite grains in the inner wall regions. A considerable change of slag composition did, in fact, take place, as shown in Table 15, particularly in the FeO, MgO, Al_2O_3 contents. For example the FeO content increased from a typical value of 0,5 per cent to as much as 15,8 per cent, while the MgO content decreased in one case from 26 per cent to 4 per cent and the Al_2O_3 content in another case increased from 1 per cent to 17 per cent. At a given slag CaO/SiO_2 ratio and temperature it can be seen from Table 15 that slags with substantially different initial MgO or Al_2O_3 contents converge upon the same final or equilibrium slag composition.

An examination of the chromite grains located near the inner surface of the crucible wall showed that considerable changes in the compositions of the edges of these grains had taken place. A summary of the data from Appendix 5 for the inner wall region is given in Table 16 which shows that the MgO content had increased from 12,4 per cent in the original unaltered chromite (see Table 13) to as much as 22,1 per cent while the maximum and minimum Al_2O_3 contents ranged from 30,6 per cent to 5,2 per cent respectively compared with the original value of 13,6 per cent. The approach to equilibrium by the slag probably consists of successive reactions between the liquid slag and the edges of chromite grains as it penetrates the porous crucible wall and flows towards the outer regions of the crucible wall. These reactions may involve both the precipitation of excess MgO and Al_2O_3 on the chromite grains and the dissolution of MgO, Al_2O_3, Cr_2O_3, FeO and Fe_2O_3 from the chromite grains until the slag composition

TABLE 15

Comparison of initial and final slag compositions

Slag no.	Composition (mass, %)											
	Initial					Final (1550°C)				Final (1650°C)			
	CaO/SiO_2	MgO	Al_2O_3	FeO	Cr_2O_3	MgO	Al_2O_3	$(FeO)_T$	Cr_2O_3	MgO	Al_2O_3	$(FeO)_T$	Cr_2O_3
5	0,03	23,1	28,8	0,8	0,02	10,1	19,1	10,9	0,8	13,6	14,9	15,9	1,3
3	0,04	18,2	24,3	0,3	0,10	9,1	19,0	12,6	0,9	15,6	14,9	13,1	1,1
6	0,07	29,4	8,9	0,5	0,02	7,3	19,2	10,5	0,5	13,1	14,5	15,8	1,0
4	0,27	26,0	18,0	0,3	0,22	4,3	17,6	13,7	0,9	6,1	15,3	14,5	1,1
2	0,40	9,8	14,4	1,0	0,02	4,8	20,2	10,5	0,9	6,3	17,4	12,4	1,0
1[A]	0,48	13,0	4,0	0,5	0,02	5,8	12,5	12,4	1,1	6,1	13,1	13,2	1,8
7	0,65	4,5	1,4	0,8	0,09	6,6	14,2	10,8	0,6	4,5	16,8	11,1	0,9

TABLE 16

Compositions of the edges of chromite grains from the crucible inner wall

Run no.	Slag no.	Composition (mass, %, normalized)						
		MgO	Al_2O_3	SiO_2	CaO	TiO_2	Cr_2O_3	$(FeO)_T$
1/4	5	21,4	29,3	0,7	0,1	0,1	38,6	9,8
2/4	4	18,9	20,7	1,0	0,1	0,2	42,1	17,1
3/4	6	19,5	15,5	0,9	0,1	0,2	48,8	15,2
8/4	7	12,5	5,2	0,2	0,6	0,2	63,5	17,8
1/5	5	22,1	30,6	0,9	0,0	0,1	41,2	5,1
2/5	6	12,7	23,8	0,7	0,1	0,2	42,1	20,5
3/5	4	17,4	26,0	0,7	0,1	0,2	40,4	15,3
8/5	7	13,2	5,6	0,6	0,4	0,1	63,1	17,0

changes sufficiently for no further reaction to take place, i.e. reach equilibrium with the chromite or become saturated with respect to the original chromite. The porous crucible therefore provides a means by which the liquid slag can react many times in succession with selected chromite which then forces the slag towards equilibrium with the original chromite. A simple mixture of excess chromite and slag in an inert crucible would converge upon a different equilibrium in which a different chromite composition from the original would be expected.

The advantages of this technique therefore include the freedom to fix the chromite composition and to vary the initial slag composition widely. The attainment of equilibrium is rapid and does not require separate lengthy tests to approach the desired equilibrium by a process of successive approximation. The limitations of the process are the inability to determine the oxidation state of the elements present so that in this particular case the relevant proportions of FeO and Fe_2O_3 in the slag could not be determined. The relatively large sample size makes rapid quenching difficult with the associated increased errors in determining the slag composition when a secondary crystal phase is formed.

This technique is useful where real systems with all the naturally occurring impurities are of interest and can provide sufficiently accurate information upon which further work, based on more traditional methods, can be carried out.

6.2 The Effects of Temperature and CaO/SiO_2 Ratio

The effect of increased temperature upon the maximum solubility of the spinel-forming species in the slag was generally as expected, i.e. an increase in solubility. Typically, as can be seen from Table 15, the MgO concentration increased by 3 per cent MgO, the FeO concentration by 2 per cent FeO and the Cr_2O_3 concentration by 0,4 per cent Cr_2O_3 with an increase in temperature from 1550°C to 1650°C. However, the alumina content of the slag decreased by about 2 per cent Al_2O_3 which was not expected. A possible reason for this behaviour may be linked to $FeO-Fe_2O_3$ equilibrium as a function of temperature. There is no data available for the complex slags of this study but it is known that the Fe^{2+}/Fe^{3+} ratio in slags is temperature dependent[40]. A change in the activity of Fe_2O_3 in the slag at the higher temperature may have a substantial influence upon the activity of Al_2O_3 since they are similar compounds. A further possibility may be the influence of temperature upon the activities of the Fe_2O_3 and FeO in the chromite spinel leading to a redistribution of the Fe^{3+} cations between the octahedral and tetrahedral sites in the lattice. This possibility exists because Fe^{3+} has the lowest octahedral site preference energy as discussed earlier (Section 2.1). A change in the Fe_2O_3 spinel activity in this way could again influence the activity of the Al_2O_3 in the spinel but probably not the Cr_2O_3, which has a much higher site preference energy compared with Al_2O_3.

The lack of information on the oxidation state of the iron in the slag phase prevents further exploration of these

possibilities. It should be noted that there was no significant loss or gain in mass during the experiments at either temperature (see Table 11) so the possibility of thermal decomposition of the Fe_2O_3 component at the higher temperatures seems unlikely. The average mass lost in the 1550°C tests was 0,03 g while an average mass gain of 0,12 g was observed in the 1650°C tests. These figures correspond to the decomposition of 4 per cent of the original Fe_2O_3 in the 1550°C tests and the oxidation of 6 per cent of the FeO in the 1650°C tests.

The effect of the CaO/SiO_2 mass ratio upon the slag composition was confined mainly to the $(FeO)_T$ and MgO contents. The Cr_2O_3 saturation solubility (~ 1,0 per cent Cr_2O_3) was not significantly affected by the change in CaO/SiO_2 ratio in the measured range from 0,03 to 0,65. The Al_2O_3 content at 1650°C increased slightly from about 15 per cent to about 17 per cent with increasing CaO/SiO_2 mass ratio. However, at 1550°C the Al_2O_3 remained constant until a CaO/SiO_2 ratio of approximately 0,3 after which it dropped from 19 per cent to about 14 per cent (see Figure 11).

The FeO and MgO contents decreased steadily with increasing CaO/SiO_2 ratio from typically 15 per cent to 12 per cent and 5 per cent respectively at 1650°C. These oxides both displayed a minimum at a SiO_2/CaO of about 0,3 in the 1550°C tests with FeO dropping to about 8 per cent from 12 per cent and recovering to 12 per cent at higher CaO/SiO_2 ratios (~ 0,55). The MgO dropped to approximately 5 per cent from an initial value (CaO/SiO_2 ~ 0,05) of 10 per cent and increased to 7 per

cent MgO at the high CaO/SiO_2 values (see Figs. 11 and 12 and Table 15).

The behaviour observed at 1650°C is consistent with increasing activity coefficients of MgO and Al_2O_3 as the slag CaO content increases due to the stronger basic nature of CaO compared with MgO and FeO. The lack of any strong effect upon the Al_2O_3 behaviour at this temperature is also consistent with the amphoteric nature of Al_2O_3. The behaviour at 1550°C of FeO, MgO and Al_2O_3 is not clear and may be related to the anomalous temperature behaviour of the Al_2O_3 as discussed above.

Since the two phases (solid chromite and liquid slag) were in equilibrium the activities of each species in each phase must be equal, by definition. Consequently if the chromite spinel can be regarded as an ideal solid solution especially at high temperatures, the activities of the spinel constituents may be calculated. Muan[21] has noted that the ideal activity composition relationship for such solid solutions containing different cation sites and stoichiometry requires some careful definition. The chromite spinel can be regarded as a solid solution of MgO and FeO on the divalent sites and of Cr_2O_3, Al_2O_3, and Fe_2O_3 on the trivalent sites. Since there are two cations involved on the trivalent sites Muan states that the activity is the square of the mole fraction in this case. Therefore the ideal activity-composition relationships used were:

$a_{Cr_2O_3} = X^2_{Cr_2O_3}$

$a_{Al_2O_3} = X^2_{Al_2O_3}$ where X_i = mole fraction of species i

$a_{Fe_2O_3} = X^2_{Fe_2O_3}$

$a_{FeO} = X_{FeO}$ and a_i = activity of species i relative to the pure solid species

$a_{MgO} = X_{MgO}$

The composition given in Table 7 was used to calculate the activities of the chromite species which yielded the following values:

$a_{Cr_2O_3} = 0,100$

$a_{Al_2O_3} = 0,017$

$a_{Fe_2O_3} = 0,002$

$a_{MgO} = 0,246$

$a_{FeO} = 0,260$

This data was then used to calculate the activity coefficients of the various species in the slag (relative to pure solid species at the same temperature). It was assumed that the Fe_2O_3 contribution was negligible simply for the purpose of obtaining some idea of the behaviour of the FeO. The activity coefficients thus calculated are shown in Table 17. The outstanding feature of the data is the high value of the activity coefficient of Cr_2O_3 in the slag (ranging from 13 to 40). This reflects the limited solubility of Cr_2O_3 in silicate slags and is consistent with the available phase diagram for the $MgO-SiO_2-Cr_2O_3$ system[41]. The influence of the additional

Table 17: Activity coefficients of MgO, Al_2O_3, (FeO) and Cr_2O_3 in chromite saturated slags

Run no.	CaO/SiO_2 (mass)	Activity coefficient			
		MgO	Al_2O_3	$(FeO)_T$	Cr_2O_3
1/5, 2/5, 4/5, 6/5	0,04	1,17	0,19	2,00	20,3
3/5	0,34	2,56	0,18	2,03	22,5
5/5	0,30	2,48	0,16	2,36	39,2
7/5	0,42	2,59	0,21	2,26	13,3
8/5	0,52	3,46	0,16	2,65	26,2
1/4, 3/4, 4/4	0,05	1,71	0,14	2,52	31,4
2/4	0,25	3,73	0,13	4,48	22,0
5/4	0,32	3,19	0,13	2,74	25,7
9/4	0,47	2,70	0,22	2,39	22,6
8/4	0,55	2,41	0,20	2,80	40,3

components FeO, Fe_2O_3, Al_2O_3 and CaO has not substantially increased the solubility of Cr_2O_3 in silicate slags. The activity coefficients for MgO and $(FeO)_T$ at 1650°C increase with increasing slag CaO/SiO_2 in accordance with expectations while the Al_2O_3 values remain approximately constant. This behaviour is in accordance with the strongly basic nature of CaO, as discussed earlier.

6.3 Implications for Chromite Smelting

This investigation set out to determine the conditions for chromite dissolution into silicate slags to assist in the selection of smelting conditions, particularly the type and quantity of fluxing additions. The use of the unaltered chromite establishes an extreme condition without regard for the reduction reactions, i.e. the slag composition required to completely dissolve chromite under inert conditions. The application of this information to the smelting process is now considered, firstly with regard to the Cr_2O_3 solubility and secondly to the MgO and Al_2O_3 solubilities.

The results of this study confirm that in a complex slag containing iron oxides as well as the usual slag-forming components (MgO, Al_2O_3, CaO, SiO_2) that the maximum solubility of Cr_2O_3 is low, typically 1 per cent Cr_2O_3 at 16[illegible]°C. Therefore, as discussed earlier, two important conditions are likely to be required to achieve rapid reduction of the Cr_2O_3 contained in the chromite spinel. Firstly strongly reducing conditions must be provided, which in a smelting furnace would exist at the slag-carbon interface and/or the slag-metal interface. Metal with more than 4 per cent carbon or 5 per

cent silicon would be capable of maintaining the Cr_2O_3 activity at 10^{-4} or less (see Tables 2 and 3) and if the activity coefficient of Cr_2O_3 is indeed ~ 26, as discussed above, then the mole fraction of Cr_2O_3 in equilibrium with such a metal would be ~ 4×10^{-6}. The second requirement is the effective mass transport (including both bulk slag movement and pure diffusion) of the dissolved Cr_2O_3 from the chromite-slag interface to the slag-metal interface. The rate of such transport processes ($N^0_{Cr_2O_3}$) has been defined by Gieiger and Poirier[42] as the product of the concentration gradient in the slag of Cr_2O_3 and the mass transport coefficient (k_M) as follows:

$$N^0_{Cr_2O_3} = k_M(C^{\infty}_{Cr_2O_3} - C^0_{Cr_2O_3})$$

Where $N^0_{Cr_2O_3}$ is the molar flux of Cr_2O_3 at the slag-metal interface (mole.$^{-2}$.5^{-1}) and $C^0_{Cr_2O_3}$ and $C^{\infty}_{Cr_2O_3}$ are molar concentrations of Cr_2O_3 (mole.m^{-3}) at the slag-metal interface and the bulk slag respectively.

The maximum concentration of Cr_2O_3 possible in the bulk slag is the saturation solubility of Cr_2O_3 and since the equilibrium Cr_2O_3 concentration at the slag-metal interface is extremely small (on thermodynamic grounds) it can be neglected, and the maximum rate of mass transport can be approximated by $N^0_{Cr_2O_3} \approx k_M C^S_{Cr_2O_3}$ where $C^S_{Cr_2O_3}$ is the equilibrium solubility of Cr_2O_3 in the slag. Since the equilibrium solubility of Cr_2O_3 has been found to be approximately an order of magnitude less than the typical solubilities of other oxides in the slag, (e.g.

FeO ~ 10 per cent cf. Cr_2O_3 ~ 1 per cent) it is clearly necessary to maximize the value of k_M to achieve mass transport rates comparable to those of FeO slags. There is no reason to expect the diffusivity of Cr_2O_3 in liquid silicate slags to be higher than that of other oxides (e.g. FeO) and therefore efforts to increase k_M in practice would probably have to be directed towards increasing the bulk slag movement by some form of stirring.

The solubility of MgO and Al_2O_3 in the slag becomes important if the required conditions for rapid reduction of Cr_2O_3 are met, because then the dissolution of the chromite spinel may be expected to become rate limiting. The spinel itself cannot dissolve in the slag completely as long as the MgO and Al_2O_3 contents of the slag exceed the solubility limits of MgO and Al_2O_3. The Cr_2O_3 and FeO can then only leave the chromite spinel by solid state diffusion within the spinel. Therefore, in order to ensure the dissolution of the entire spinel, SiO_2 and/or CaO fluxes should be added to lower the MgO and Al_2O_3 contents in the slag to below their solubility limits. The Al_2O_3 limit found at 1650°C was typically 15 to 17 per cent Al_2O_3 (see Table 15) and is not significantly affected by the CaO/SiO_2 ratio selected. The MgO solubility value is, however, raised drastically (from 6 per cent to 13 per cent) at CaO/SiO_2 less than 0,1 and therefore lower values of CaO/SiO_2 should be selected where possible. These limits are the worst case and should be regarded as the lower solubility limits for flux addition calculations. The upper limit is given by the solubility of a pure $MgO.Al_2O_3$ spinel where, from the known

phase diagram[11] at 1650°C ... the absence of CaO, MgO levels of 25 per cent to 30 per cent can be tolerated together with Al_2O_3 contents of 30 per cent to 35 per cent. The selection of the optimum level of flux addition in practise requires a balance between the cost of the energy requirement to melt the flux and the benefits obtained by higher smelting rates and lower losses of unreduced chromite in the discard slag.

Industrial practise typically utilizes slags with MgO and Al_2O_3 contents of 20 per cent MgO and 25 per cent Al_2O_3[6] at a CaO/SiO_2 ratio of ~ 0,25 which are much higher than the saturation values at 1650°C of 6 per cent and 16 per cent respectively. It may, therefore, be expected that any chromite entering such a slag would not dissolve even if the conditions for rapid reduction of Cr_2O_3 were met. This is a likely mechanism for the losses of undissolved and partly reacted chromite in such slags. A means of preventing the chromite particles from by-passing the initial fluxing stage is required to reduce such losses. Possibly the addition of fluxes to the agglomerated feed (where used), i.e. briquettes, could be useful in this regard. The formation of a chromite-flux sinter as used by Fukagawa and Shimoda[33] in their experiments may be another means of ensuring that all the chromite particles are adequately fluxed.

7 CONCLUSIONS

7.1. The compositions of silicate slags in equilibrium in a Transvaal chromite (from the LG-6 layer of the Bushveld

Complex) were determined at 1550°C and at 1650°C over a range of CaO/SiO_2 ratios from 0,03 to 0,55.

7.2. The porous crucible technique developed provided a relatively rapid means of determining the equilibrium slag composition relative to an unaltered naturally occurring chromite.

7.3. The Cr_2O_3 solubility ranged from 0,5 per cent to 1,8 per cent with an average value of 1,0 per cent. A small increase in solubility from 1550°C to 1650°C of 0,4 per cent was observed. No measurable effect of the CaO/SiO_2 ratio was observed.

7.4. The MgO solubility varied from 4,3 per cent to 15,6 per cent and was affected by both temperature and CaO/SiO_2 ratio. The average solubility at 1550°C was 6,9 per cent while at 1650°C it was 9,3 per cent. The solubility was seen to be higher at CaO/SiO_2 ratio <0,1 compared with ratios between 0,1 and 0,55, i.e. 8,8 per cent cf. 5,4 per cent at 1550°C and 14,1 per cent cf. 5,8 per cent at 1650°C.

7.5. The Al_2O_3 solubility varied from 12,5 per cent to 20,2 per cent with an average value of 17,4 per cent at 1550°C and 15,3 per cent at 1650°C. No clear effect of CaO/SiO_2 ratio was evident.

7.6. The total iron expressed as FeO varied from 10,5 per cent to 15,9 per cent with an average value of 11,6 per cent at 1550°C and 13,7 per cent at 1650°C. The solubility at 1650°C was higher (14,3 per cent) at CaO/SiO_2 ratios of

<0,1 than for ratios between 0,1 and 0,55 (12,8 per cent).

7.7. The low solubility of Cr_2O_3 in these slags (~ 1,0 per cent) suggests that strongly reducing ($P_{O_2} < 10^{-15}$ atm.) and well stirred slag conditions would be required to ensure the rapid dissolution of the chromite.

7.8. A further limitation to rapid dissolution may be expected if the MgO and Al_2O_3 contents of the slag exceed 6 per cent and 16 per cent respectively at the usual CaO/SiO_2 ratio of 0,25.

8 RECOMMENDATIONS

8.1. The use of fluxes containing MgO and Al_2O_3 in the smelting of chromite should be minimized to increase throughput and chromium recovery within the constraints of an acceptable slag liquidus temperature and electrical conductivity.

8.2. The lowest possible CaO/SiO_2 ratio should be utilized within the same constraints as 8.1 but, in addition, the constraints of slag viscosity (increased entrainment of metal blebs in the slag) and alloy sulphur content should be considered.

8.3. Further work to quantify the beneficial effects of utilizing Na_2O and CaF_2 for the fluxing of chromite which were identified by Dawson and Edwards[32] using the porous chromite crucible technique should be undertaken, with a

view towards developing a low temperature (~ 1450°C) smelting technique.

8.4. Further work to examine the role of slag composition in the smelting of chromite should be undertaken. A rotating cylinder of chromite in a graphite crucible containing various slags is recommended. The reaction rate could be followed by monitoring the off-gas or possibly by a gravimetric method. This investigation should clarify under which conditions chromite dissolution, transport of chromium oxides through the slag or chemical reaction at the graphite interface become the rate limiting step.

APPENDIX 1

CALCULATION OF THE ACTIVITIES OF VARIOUS CHROMIUM OXIDE COMPOUNDS IN EQUILIBRIUM WITH Fe-Cr-C AND Fe-Cr-Si ALLOYS

1. Fe-Cr-Si Alloys

Equations to be considered

$$^3/_2\ \underline{Si} + (Cr_2O_3) = 2\ \underline{Cr} + {}^3/_2\ (SiO_2) \qquad \text{Equ.11}$$

$$\tfrac{1}{2}\ \underline{Si} + (CrO) = \underline{Cr} + \tfrac{1}{2}\ (SiO_2) \qquad \text{Equ.12}$$

$$^3/_2\ \underline{Si} + MgCr_2O_4(s) = 2\underline{Cr} + (MgO) + {}^3/_2(SiO_2) \qquad \text{Equ.13}$$

$$\underline{Si} + O_2(g) = (SiO_2) \qquad \text{Equ.14}$$

Assume:
(a) temperature constant 1600°C
(b) activity of MgO in slag phase = 0,17[12]
(c) activity of SiO_2 in slag phase = 0,40
(d) activity of Cr in alloy phase = 0,40
(e) pressure = 1,0 atmosphere (inert)
(f) all activities are relative to the pure species at 1600°C.

$$\frac{a_{Cr}^2 \cdot (a_{SiO_2})^{3/2}}{a_{Cr_2O_3} \cdot (a_{Si})^{3/2}} = K_{11} = 1{,}179 \times 10^6 \quad \text{Barin \& Knacke}^{24}$$

$$\frac{a_{Cr}^2 \cdot (a_{SiO_2})^{3/2} \cdot a_{MgO}}{(a_{Si})^{3/2} \cdot a_{MgCr_2O_4}} = K_{13} = 1{,}108 \times 10^4 \quad \text{Barin \& Knacke}^{24}$$

$$\frac{a_{SiO_2}}{P_{O_2} \cdot a_{Si}} = K_{14} = 1{,}178 \times 10^{16} \quad \text{Barin \& Knacke}^{24}$$

$\Delta G°$, for Equ. 12 = -17,54 kcal/mole CrO using $\Delta G°$ data for CrO from Toker[25], remaining data from Barin and Knacke[24].

$$\therefore \ln K_{12} = \frac{-\Delta G^{\circ}_{12}}{RT} = \frac{-17,54}{1,987 \times 1,873}$$

$$\therefore \frac{a_{Cr} \cdot (a_{SiO_2})^{\frac{1}{2}}}{(a_{Si})^{\frac{1}{2}} a_{CrO}} = K_{12} = 1,112 \times 10^{2}$$

$$a_{Si} = \gamma_{Si} \cdot X_{Si}$$

$$\ln \gamma_{Si} = \ln \gamma^{\circ}_{Si} + \epsilon^{Si}_{Si} X_{Si} + \epsilon^{Cr}_{Si} X_{Cr}$$

$$= -6,645 + 25,21 X_{Si} + 0,197 X_{Cr} \quad \text{...Sigworth \& Elliott}^{43}$$

Assuming that the activity of silicon can be approximated by the data for dilute iron alloys, since chromium and iron behave almost ideally towards each other, and that the alloy contains a constant 50 per cent chromium by mass, the silicon activities can be calculated for the following alloy compositions.

% Si	X_{Si}	X_{Cr}	$\ln \epsilon_{Si}$	a_{Si}
5,0	0,092	0,494	-4,23	$1,34 \times 10^{-3}$
0,5	0,010	0,516	-6,29	$1,85 \times 10^{-5}$
0,05	0,001	0,518	-6,52	$1,48 \times 10^{-6}$

The use of these silicon activities together with the assumed activities of chromium in the metal, silica and magnesia in the slag in the expression for the equilibrium constants shown above allow an estimate to be made of the activities of Cr_2O_3, CrO and $MgCr_2O_4$ in equilibrium with Fe-Cr-Si alloys of the above compositions. The oxygen partial pressure in these systems can also be calculated.

2. Fe-Cr-C Alloys

Equations to be considered

$\underline{C} + \frac{1}{2}\ O_2(g) = CO(g)$ Equ. 7

$3\underline{C} + (Cr_2O_3) = 2\underline{Cr} + 3CO(g)$ Equ. 2

$\underline{C} + (CrO) = \underline{Cr} + CO(g)$ Equ. 6

$3\underline{C} + MgCr_2O_4(s) = 2\underline{Cr} + (MgO) + 3CO(g)$ Equ. 5

Assume:
(a) temperature constant at 1600°C
(b) pressure constant at 1,0 atmospheres of CO
(c) all activities relative to the pure species at 1600°C
(d) a constant 50 per cent by mass chromium in the alloy
(e) a constant MgO activity of 0,17 in the slag.

$\frac{P_{CO}}{a_c \cdot (P_{O_2})^{\frac{1}{2}}} = K_7 = 4,794 \times 10^7$ Barin & Knacke[24]

$\frac{(a_{Cr})^2 \cdot (P_{CO})^3}{(a_C)^3 \cdot (a_{Cr_2O_3})} = K_2 = 1,326 \times 10^5$ Barin & Knacke[24]

$\frac{a_{Cr} \cdot P_{CO}}{a_C \cdot a_{CrO}} = K_6 = 49,24$ Barin & Knacke[24] and Toker[25] for CrO data

$\frac{(a_{Cr})^2 \cdot a_{MgO} \cdot (P_{CO})^3}{(a_C)^3 \cdot a_{MgCr_2O_4}} = K_5 = 1,671 \times 10^3$ Barin & Knacke[24]

The activities of chromium and carbon have recently been calculated by Healy[26] and combining this information with the above equilibrium equations the effect of varying carbon contents on the activities of chromium oxide compounds in the slag may be estimated. The oxygen partial pressure variations are also calculated for comparison.

APPENDIX 2

DETAILS OF THE EXPERIMENTAL EQUIPMENT

A schematic diagram of the vertical tube furnace and the associated equipment is shown in Figure A-1. The position of the crucible in the hot zone of the furnace is shown together with the other important dimensions in Figure A-2. The electrical power supply connections were made through the bottom of the furnace by means of high temperature electrically insulating connectors. The purge gas to the furnace shell, to protect the molybdenum wire heating element from oxidation, was supplied through an alumina tube positioned close to the windings and discharging near the middle of the furnace.

The heating element was designed using recommended values by Finn[44] for the voltage drop per turn (2 to 3 V/turn) and the power to surface area ratio of the wire (7 to 18 W/cm^2). The data of Bockris[45] was used to estimate the resistivity of the molybdenum wire as a function of temperature (see Figure A-3). The large increase in resistivity (approximately ten fold) from room temperature to a working temperature of 1800°C requires a power supply with a wide range of current and voltage to meet both warm-up and high temperature demands. Although thermal losses radially through the shell were estimated at only 2,1 kW it was decided to make provision for up to 5 kW because of the uncertain extent of the end-zone heat losses. Previous work on a similar type of furnace by Toker[25] made allowance for a 50 per cent increase in furnace power because of end-zone losses. This design utilizes a much larger work tube diameter to length ratio then Toker (0,086

cf. 0,052) which may be expected to increase the proportion of end-zone losses. A thyristor power supply with a 40 A x 220 V power rating was therefore selected.

The element winding pattern used is shown in Figure A-4 together with details of the wire and tube diameters. The winding was coated with an alumina cement (TR1-MORE PURE) to just cover the wire (< 0,3 mm), oven dried at 120°C and fired at 600°C to secure the cement and winding firmly in position. The furnace was warmed-up slowly over a period of five to seven days to avoid thermal shock, especially of the recrystallized alumina tubes. Considerable care was required to ensure the integrity of the furnace seals at the operating temperature. Furnace life-times varied considerably and at temperatures of 1650°C not more than three weeks of working life could be expected.

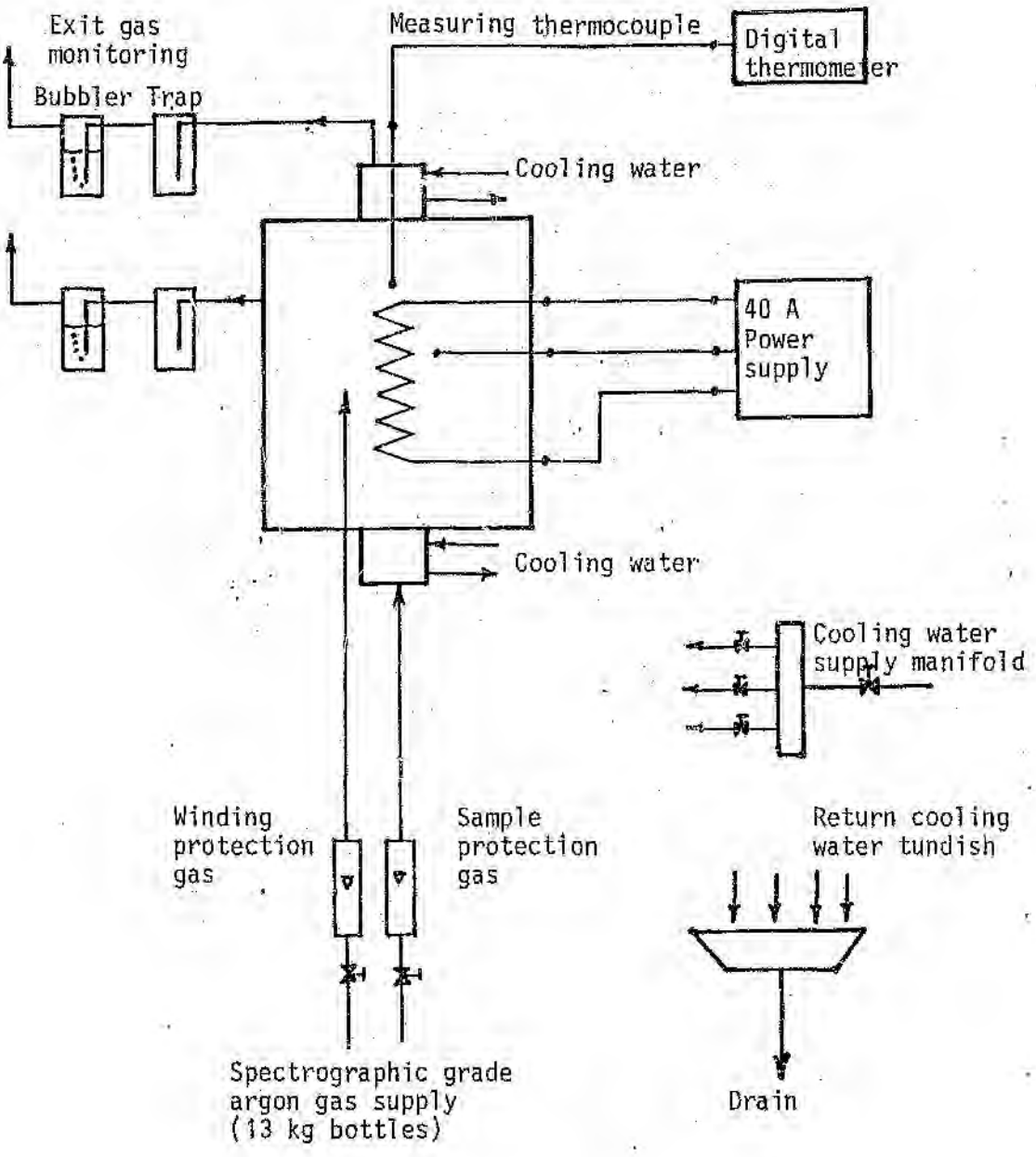


Figure A-1. Schematic diagram of the vertical tube furnace facility

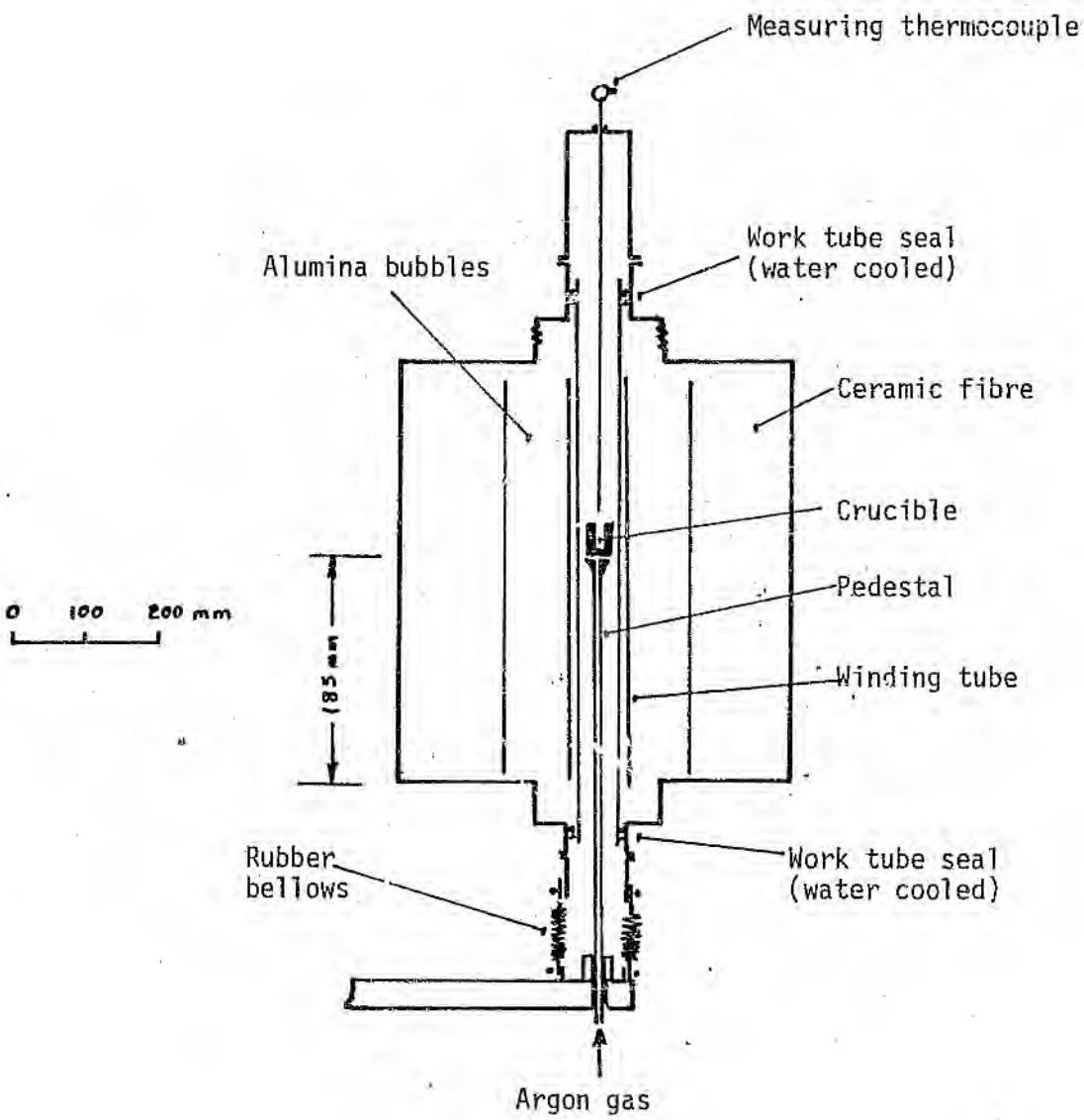


Figure A-2. Location of the crucible in the furnace

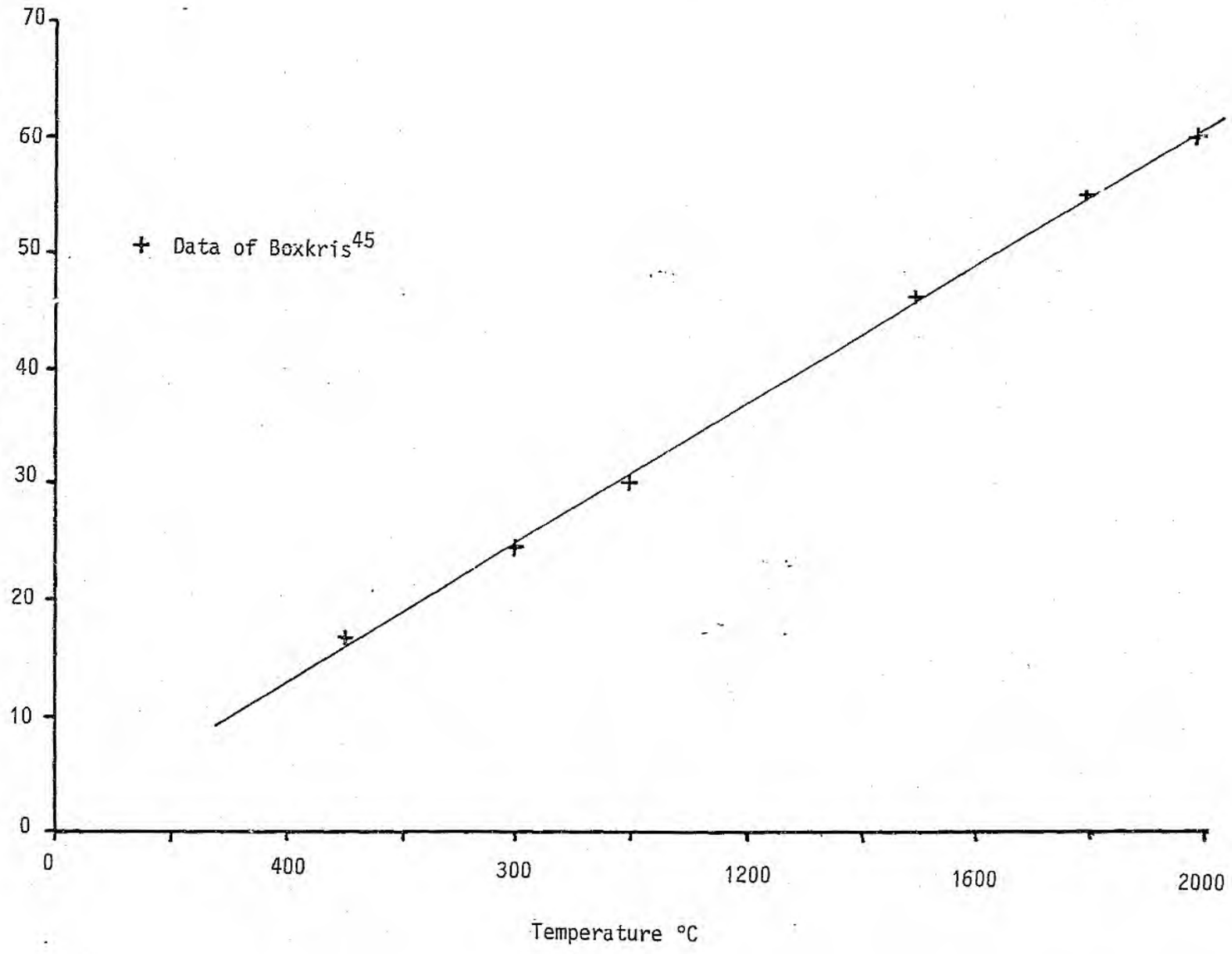
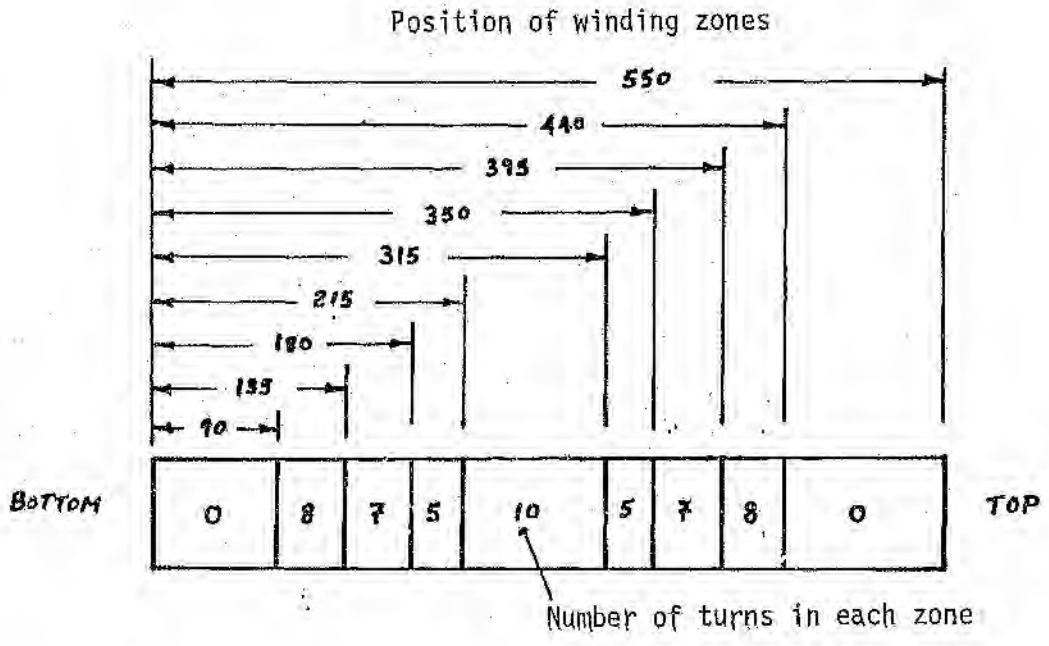


Figure A-3. Resistivity of molybdenum



Data:			
	Molybdenum wire diameter	=	1,0 mm
	Winding tube diameter	=	76 ± 1 mm
	Wire length	=	11,9 m
	Total number of turns	=	50
	Winding tube material	=	recrystallized alumina
	Cement	=	TRI-MORE pure
	Water	=	Deionized
	Firing temperature	=	600°C

Figure A-4. Molybdenum heating element, winding pattern

APPENDIX 3

CALIBRATION OF REFERENCE THERMOCOUPLE

Council for Scientific and Industrial Research

National Measuring Standards and Metrology Division
National Physical Research Laboratory

P O Box 395 Pretoria 0001-South Africa
Telex 3 - 21312 SA Telegrams: Navorsfis

Tel: National (012)86-9211 ext 3439
International + 27 12 86-9211

CERTIFICATE OF CALIBRATION

No:13144/Met/Temp

Calibration of:	TYPE-B THERMOCOUPLE WIRE
Manufacturer:	-
Model No:	-
Serial No:	WR 4-86
Calibrated for:	Council For Mineral Technology Randburg Tvl.
Calibration procedure:	T8-E1
Date of Calibration:	June 1986
Expiry Date:	-
Calibrated by:	D J Smuts
Checked by:	R F Smith
No. of pages:	7

for Chief Director

2 T8-E1

CALIBRATION OF A THERMOCOUPLE TYPE B
SERIAL NO: WB 4-86

The thermocouple was calibrated at 18 different points over the range 0°C - 1750°C

In the equation:

$$Emf = a_0 + a_1 t + \ldots + a_n t^n \quad (\text{where } n = 8)$$

The following values were obtained for the constants:

a_0 =-2.6861231E-04 mV
a_1 =-2.1032806E-04 mV * °C^{-1}
a_2 = 5.3075572E-06 mV * °C^{-2}
a_3 = 1.8948983E-09 mV * °C^{-3}
a_4 =-6.5138172E-12 mV * °C^{-4}
a_5 = 8.7564988E-15 mV * °C^{-5}
a_6 =-6.5515077E-18 mV * °C^{-6}
a_7 = 2.5511919E-21 mV * °C^{-7}
a_8 =-4.0673059E-25 mV * °C^{-8}

Using these constants an emf - temperature table has been computed and is attached to the certificate.

Uncertainty of the calibration: ±1 K between 0 and 1150 °C
±0.2% between 1150 and 1600 °C
±0.3% between 1600 and 1750 °C

The uncertainty is estimated in terms of 99.7% confidence limits.

No: 13144/Met/Temp
Date of calibration: June 1986
Calibrated by:
Checked by:

for Chief Director

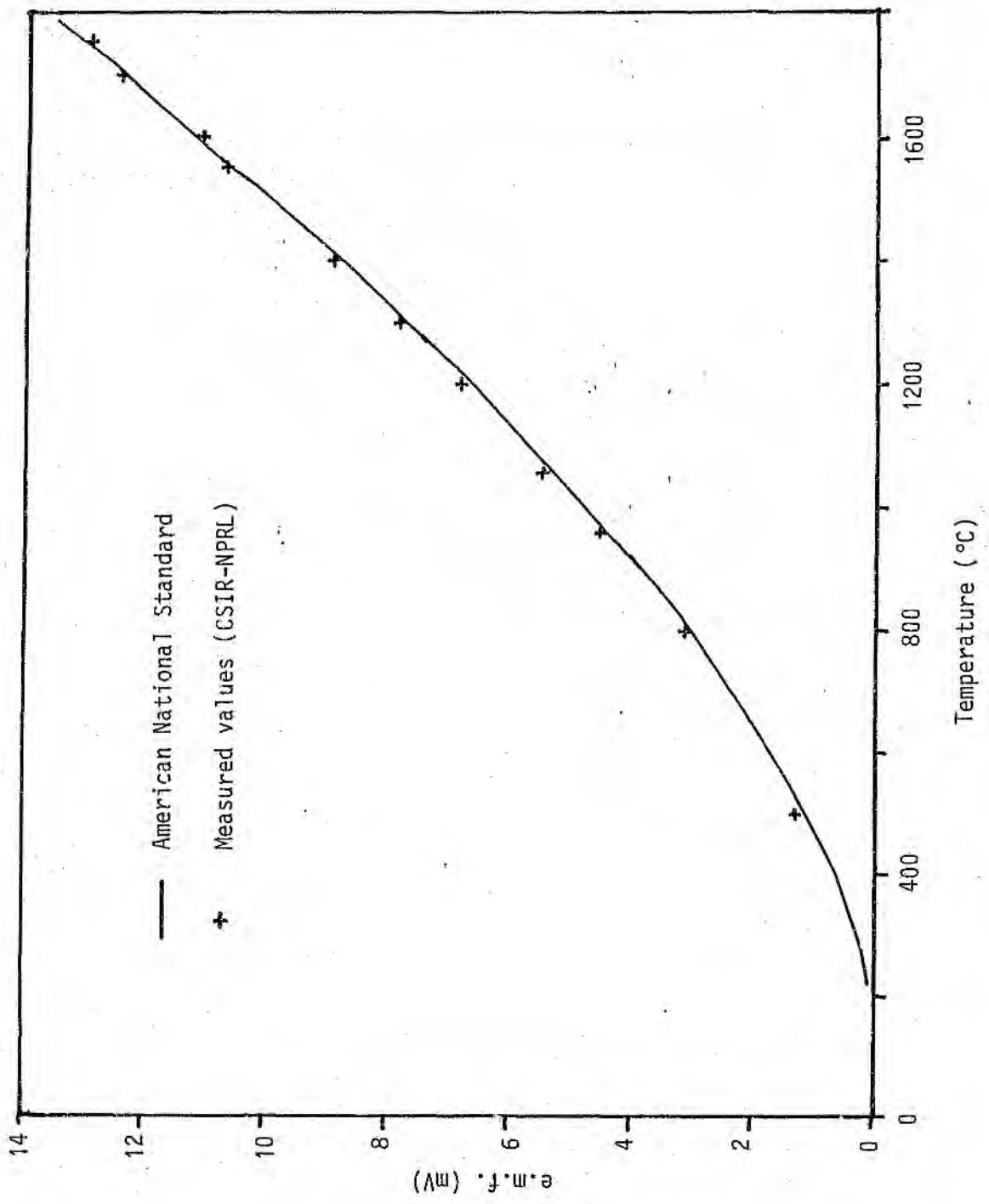


Figure A-5. Comparison of calibrated thermocouple with American National Standard data

10-Jul-86

VALUES USED FOR TEMPERATURES & EMFs
INSTRUMENT SERIAL NO:WB 4-86

T(1) =	0.01	V(1) =	-0.0002
T(2) =	19.967	V(2) =	-0.0024
T(3) =	49.9721	V(3) =	0.0026
T(4) =	122.282	V(4) =	0.0557
T(5) =	231.9681	V(5) =	0.24625
T(6) =	419.58	V(6) =	0.8675
T(7) =	500	V(7) =	1.240826
T(8) =	630.755	V(8) =	1.976
T(9) =	800	V(9) =	3.14911
T(10) =	961.93	V(10) =	4.48555
T(11) =	1064.43	V(11) =	5.42835
T(12) =	1200	V(12) =	6.776353
T(13) =	1300	V(13) =	7.834981
T(14) =	1400	V(14) =	8.939463
T(15) =	1554	V(15) =	10.705
T(16) =	1600	V(16) =	11.23968
T(17) =	1700	V(17) =	12.39164
T(18) =	1750	V(18) =	12.95015

Rsquare = 1
Polynomial degree = 8

APPENDIX 4

DETAILS OF THE EXPERIMENTAL TEST RUNS

1. Runs at a nominal temperature of 1550°C

Nine acceptable test runs were performed at this temperature. Details of the furnace temperature calibration were as follows:

	Reference Thermocouple	Measuring Thermocouple
Bottom of empty crucible	1548°C	-
Middle of empty crucible	1550°C	-
Top of empty crucible	1551°C	-
Normal measuring position, i.e. 10 mm above top of crucible	1552°C	1554°C

It was assumed that the actual temperatures in the centre of the crucible during the subsequent test runs could be estimated from the indicated value obtained from the measuring thermocouple by applying the following corrections:

(i) error relative to reference thermocouple 2°C (high)

(ii) error due to position of measuring thermocouple 2°C (high)

Accordingly all temperature readings taken during the subsequent tests were reduced by 4°C.

The details of the runs are shown in Table A-1.

2. Runs at a nominal temperature of 1650°C

Furnace temperature calibration

	Reference Thermocouple	Measuring Thermocouple
Bottom of crucible	1644°C	-
Middle of crucible	1647°C	-
Top of crucible	1647°C	-
Measuring position (10 mm above top of crucible)	1649°C	1648°C

Estimated actual temperature at middle of crucible in subsequent test runs relative to the indicated temperature by the measuring thermocouple corrected by:

(i) Error relative to reference = 1°C (low)

(ii) Error due to measuring position = 2°C (high)

All measurements were therefore reduced by 1°C in reporting the subsequent runs.

Details of the runs are presented in Table A-2.

TABLE A-1

Details of test runs at 1550°C

Run no.	Date	Slag no.	Chromite mass in(g)	Slag mass in (g)	Chromite and slag out (g)	Time at Temperature h	Temperature		Average	
							Min. °C	Max. °C	Current A	Voltage V
1/4	87.02.19	5	93,44	22,70	115,97	2,3	1544	1548	14,5	148
2/4	87.02.19	4	94,32	23,23	117,53	9,8	1544	1548	14,5	143
3/4	87.02.20	6	92,94	23,78	116,68	1,0	1546	1552	14,5	148
4/4	87.02.20	3	92,13	23,70	115,87	1,0	1551	1557	No steady readings	
5/4	87.02.20	2	91,63	21,98	113,68	1,0	1557	1564	No steady readings	
6/4	87.02.20	4	89,92	22,47	112,30	1,0	1557	1562	No steady readings	
7/4	87.02.21	3	88,72	23,25	112,41	8,1	1549	1559	No steady readings	
8/4	87.02.21	7	90,29	21,40	111,75	0,9	1551	1558	14,5	141
9/4	87.02.21	1[A]	92,24	23,90	116,15	1,0	1548	1558	14,5	138

TABLE A-2

Details of test runs at 1650°C

Run no.	Date	Slag no.	Chromite mass in(g)	Slag mass in (g)	Chromite and slag out (g)	Time at Temperature h	Temperature		Average	
							Min. °C	Max. °C	Current A	Voltage V
1/5	87.02.22	5	92,80	25,22	118,02	1,0	1652	1658	16,0	166
2/5	87.02.22	6	94,57	25,32	119,99	1,0	1647	1654	15,8	165
3/5	87.02.22	4	92,11	22,40	114,43	1,0	1647	1654	15,7	160
4/5	87.02.22	3	93,80	23,31	117,00	1,0	1647	1651	16,0	160
5/5	87.02.22	2	93,18	21,50	114,53	1,0	1650	1656	16,0	160
6/5	87.02.23	5	93,33	21,67	114,48	11,0	1647	1653	16,0	159
7/5	87.02.23	1[A]	93,03	26,74	119,76	1,0	1643	1646	16,0	161
8/5	87.02.23	7	93,60	22,88	116,31	1,0	1650	1658	15,8	146

APPENDIX 5

DETAILED RESULTS OF MICRO-ANALYSES

TABLE A-3

Detailed results of microanalyses for each run

Run no. 1/4

Position : Inner wall Equipment : SEM Total : Normalized
Sample no.: AW 603 Polaroid no.: 04123

Point description	Composition (mass, %)						
	MgO	Al_2O_3	SiO_2	CaO	TiO_2	Cr_2O_3	FeO
Altered edge 1	21,17	26,34	0,77	0,06	0,00	42,15	9,52
Altered edge 2	21,80	32,28	0,69	0,02	0,10	35,47	9,64
Altered edge 3	21,09	29,29	0,63	0,17	0,26	38,25	10,36
Centre	19,21	20,14	0,86	0,14	0,31	49,64	9,69
Slag crystalline, 75%	23,28	16,38	52,69	0,49	0,39	0,79	5,98
Slag matrix, 25%	7,15	21,34	59,56	3,12	0,48	0,86	7,49

Position : Outer wall Equipment : SEM Total : Not normalized
Sample no.: AW 603

Point description	Composition (mass, %)							
	MgO	Al_2O_3	SiO_2	CaO	TiO_2	Cr_2O_3	FeO	Total
Unaltered centre 1	12,58	14,51	0,00	0,11	0,23	42,28	21,87	91,58
Unaltered centre 2	12,57	14,68	0,13	0,00	0,18	43,44	22,62	93,62
Unaltered edge 1	12,82	15,28	0,34	0,00	0,10	43,12	22,59	94,25
Unaltered edge 2	12,85	15,28	0,30	0,17	0,17	42,63	23,01	94,41
Slag matrix 100% 1	9,52	17,98	55,03	1,57	1,80	0,91	10,26	97,07
Slag matrix 100% 2	10,32	19,72	54,96	1,72	1,65	0,80	11,25	100,22

Run no. 2/4

Position : Inner wall Equipment : SEM Total : Normalized
Sample no.: AW 602 Polaroid no.: 04119

Point description	Composition (mass, %)						
	MgO	Al_2O_3	SiO_2	CaO	TiO_2	Cr_2O_3	FeO
Altered edge 1	19,07	19,37	0,67	0,11	0,20	43,53	17,07
Altered edge 2	18,13	19,72	0,91	0,04	0,17	43,54	17,50
Altered edge 3	19,52	22,97	1,26	0,18	0,15	39,28	16,64
Centre	18,87	15,43	0,97	0,07	0,48	48,01	16,18
Slag crystalline 80%	15,96	11,44	49,10	11,76	0,78	0,61	10,34
Slag matrix 20%	3,51	20,17	55,26	12,17	0,85	0,71	7,32

Position : Outer wall Equipment : Probe Total : Not normalized
Sample no.: AW 602 Polaroid no.: 0087

Point description	Composition (mass, %)							
	MgO	Al_2O_3	SiO_2	CaO	TiO_2	Cr_2O_3	FeO	Total
Unaltered centre 1	11,20	15,31	0,01	0,00	0,28	47,75	25,65	100,21
Unaltered centre 2	11,16	15,27	0,00	0,03	0,21	47,56	25,55	99,80
Unaltered edge 1	11,14	14,24	0,01	0,08	0,23	47,96	25,69	99,36
Unaltered edge 2	11,03	14,24	0,00	0,10	0,33	47,58	25,72	99,00
Slag matrix 100% 1	3,76	20,77	51,76	12,34	3,71	1,33	5,88	99,75
Slag matrix 100% 2	3,51	20,69	51,95	12,11	3,44	1,07	5,52	98,55

Position : Outer wall Equipment : SEM Total : Not normalized
Sample no.: AW 602

Point description	Composition (mass, %)							
	MgO	Al_2O_3	SiO_2	CaO	TiO_2	Cr_2O_3	FeO	Total
Unaltered centre 1	11,47	13,81	0,34	0,14	0,28	46,04	23,99	97,07
Unaltered centre 2	12,33	14,09	0,38	0,07	0,20	47,13	23,90	98,02
Unaltered edge 1	12,22	13,60	0,13	0,27	0,25	45,60	23,97	96,04
Unaltered edge 2	12,58	13,68	0,34	0,00	0,32	46,04	23,58	96,54
Slag matrix 100% 1	4,03	19,30	47,70	13,15	3,37	0,85	6,44	94,84
Slag matrix 100% 2	4,25	19,59	46,89	13,88	3,18	0,85	7,01	94,65

Run no. 3/4

Position : Inner wall Equipment : SEM Total : Normalized
Sample no.: AW 601 Polaroid no.: 04118

Point description	Composition (mass, %)						
	MgO	Al_2O_3	SiO_2	CaO	TiO_2	Cr_2O_3	FeO
Altered edge 1	19,63	16,91	0,58	0,12	0,31	46,98	15,48
Altered edge 2	19,95	16,48	1,05	0,00	0,17	46,87	15,48
Altered edge 3	18,77	12,96	0,95	0,15	0,16	52,54	14,54
Altered centre	18,72	16,21	0,44	0,00	0,31	47,77	16,55
Slag crystalline 50%	48,18	0,85	44,65	0,32	0,01	0,90	5,08
Slag matrix 50%	8,89	15,41	61,82	6,05	0,36	1,08	6,38

Position : Outer wall Equipment : Probe Total : Not normalized
Sample no.: AW 601

Point description	Composition (mass, %)							
	MgO	Al_2O_3	SiO_2	CaO	TiO_2	Cr_2O_3	FeO	Total
Unaltered centre 1	11,29	14,93	0,00	0,00	0,43	47,94	26,96	101,55
Unaltered centre 2	11,12	14,44	0,02	0,00	0,55	46,96	26,08	99,17
Unaltered edge 1	10,83	13,86	0,02	0,04	0,28	47,34	27,19	99,57
Unaltered edge 2	10,74	13,90	0,01	0,02	0,19	47,60	26,23	98,70
Slag matrix 100% 1	7,52	19,09	55,41	4,44	2,36	0,52	10,25	99,84
Slag matrix 100% 2	7,15	19,09	55,34	4,28	2,16	0,55	10,26	99,50

Run no. 4/4

Position : Outer wall Equipment : Probe Total : Not normalized
Sample no.: AW 614 Polaroid no.: 0095

Point description	Composition (mass, %)							
	MgO	Al_2O_3	SiO_2	CaO	TiO_2	Cr_2O_3	FeO	Total
Unaltered centre 1	10,64	14,78	0,00	0,00	0,43	46,68	25,04	97,58
Unaltered centre 2	10,45	14,87	0,00	0,00	0,40	46,94	25,36	98,06
Unaltered edge 1	10,53	15,79	0,25	0,00	0,11	46,05	26,80	99,59
Unaltered edge 2	10,33	15,24	0,02	0,02	0,19	47,57	25,87	99,24
Slag matrix 100% 1	10,07	18,93	53,00	1,95	0,74	0,97	13,25	98,99
Slag matrix 100% 2	9,73	18,70	53,73	2,00	0,72	0,86	13,29	99,16

Run no. 5/4

Position : Outer wall Equipment : Probe Total : Not normalized
Sample no.: AW 615 Polaroid no.: 0099

Point description	Composition (mass, %)							
	MgO	Al_2O_3	SiO_2	CaO	TiO_2	Cr_2O_3	FeO	Total
Unaltered centre 1	10,65	15,22	0,00	0,06	0,30	48,44	25,95	100,67
Unaltered centre 2	10,83	15,10	0,00	0,02	0,40	48,00	26,16	100,52
Unaltered edge 1	10,68	13,95	0,06	0,17	0,18	49,33	25,83	100,26
Unaltered edge 2	10,69	14,28	0,00	0,18	0,21	49,14	25,63	100,18
Slag matrix 70% 1	3,33	21,71	48,42	12,94	1,49	0,92	11,02	99,98
Slag matrix 70% 2	3,09	21,73	49,26	13,09	1,31	0,88	9,40	98,94
Slag crystalline 30% 1	8,13	16,21	41,54	20,11	1,54	0,96	10,04	98,55
Slag crystalline 30% 2	8,43	15,93	40,76	19,48	1,72	0,77	11,51	95,67

Run no. 6/4

Position : Outer wall Equipment : SEM Total : Not normalized
Sample no.: AW 612

Point description	Composition (mass, %)							
	MgO	Al_2O_3	SiO_2	CaO	TiO_2	Cr_2O_3	FeO	Total
Unaltered centre 1	12,18	14,11	0,00	0,07	0,48	44,27	24,53	95,64
Unaltered centre 2	11,97	14,24	0,19	0,00	0,52	46,89	23,77	97,58
Unaltered edge 1	12,25	14,81	0,32	0,21	0,50	47,37	23,46	98,92
Unaltered edge 2	12,17	14,92	0,19	0,17	0,63	47,57	23,75	99,40
Slag crystalline 75% 1	18,28	9,92	47,55	10,42	0,63	0,70	13,71	101,21
Slag crystalline 75% 2	15,70	11,99	45,54	12,43	0,80	0,34	13,71	100,51
Slag matrix 25% 1	0,78	17,68	43,36	10,02	0,91	0,91	20,82	94,31
Slag matrix 25% 2	1,15	17,51	45,09	10,33	0,89	0,89	19,48	95,13

Run no. 7/4

Position : Outer wall Equipment : PHOBE Total : Not normalized
Sample no.: AW 616 Polaroid no.: 0000

Point description	Composition (mass, %)							
	MgO	Al_2O_3	SiO_2	CaO	TiO_2	Cr_2O_3	FeO	Total
Unaltered centre 1	11,00	14,13	0,00	0,02	0,14	48,00	26,13	99,43
Unaltered centre 2	10,88	14,34	0,00	0,00	0,23	47,51	26,28	99,26
Unaltered edge 1	10,53	13,68	0,06	0,03	0,17	47,28	26,98	98,81
Unaltered edge 2	10,38	13,96	0,06	0,02	0,15	46,42	26,42	97,43
Slag matrix 100% 1	7,88	18,37	54,18	2,16	1.77	0,73	11,45	96,68
Slag matrix 100% 2	7,97	17,94	54,11	2,20	1,68	0,72	11,21	96,01

Run no. 8/4

Position : Inner wall Equipment : SEM Total : Normalized
Sample no.: AW 600 Polaroid no.: 4115

Point description	Composition (mass. %)						
	MgO	Al_2O_3	SiO_2	CaO	TiO_2	Cr_2O_3	FeO
Altered edge 1	11,46	4,69	0,22	0,59	0,23	64,63	17,67
Altered edge 2	12,95	5,65	0,00	0,33	0,09	63,53	17,45
Altered edge 3	12,58	5,21	0,58	0,74	0,24	62,39	18,26
Altered centre	15,91	15,00	0,38	0,26	0,71	48,00	19,74
Slag crystalline 50%	8,78	7,95	47,87	25,91	0,50	1,04	7,95
Slag matrix 50%	0,01	8,99	49,36	38,87	0,19	0,65	1,94

Position : Outer wall Equipment : Probe Total : Not normalized
Sample no.: AW 600 Polaroid no.: 0085

Point description	Composition (mass, %)							
	MgO	Al_2O_3	SiO_2	CaO	TiO_2	Cr_2O_3	FeO	Total
Unaltered centre 1	10,99	14,08	0,04	0,12	0,47	47,24	26,40	99,34
Unaltered centre 2	11,10	14,42	0,03	0,11	0,39	47,36	26,37	99,79
Unaltered edge 1	10,70	12,07	0,07	0,25	0,23	49,13	25,47	97,92
Unaltered edge 2	10,59	10,23	0,34	0,36	0,15	50,70	24,94	97,33
Slag crystalline 80% 1	8,13	13,74	41,38	22,72	1,00	0,67	11,84	99,49
Slag crystalline 80% 2	8,13	13,67	40,70	22,62	1,13	0,51	12,31	99,08
Slag matrix 20% 1	0,38	15,85	50,52	27,67	0,56	0,45	5,29	101,43
Slag matrix 20% 2	0,39	15,74	49,75	26,90	0,75	0,43	5,23	99,53

Run no. 9/4

Position : Outer wall Equipment : SEM Total : Normalized
Sample no.: AW 601 Polaroid nos: 04131 and 04130

Point description	Composition (mass, %)						
	MgO	Al_2O_3	SiO_2	CaO	TiO_2	Cr_2O_3	FeO
Unaltered centre 1	11,88	14,99	0,78	0,08	0,57	47,00	24,70
Unaltered centre 2	10,88	13,28	0,43	0,30	0,29	50,46	24,37
Unaltered edge 1	10,80	14,18	0,13	0,18	0,33	49,80	24,58
Unaltered edge 2	11,15	12,38	0,90	0,20	0,27	50,56	24,54
Slag crystalline 80%	7,04	11,61	43,94	23,27	1,05	1,28	11,82
Slag matrix 20%	0,73	16,00	48,77	11,98	0,61	0,53	14,86

Position : Upper wall (no slag contact) Equipment : SEM Total : Not normalized
Sample no.: AW 665

Point description	Composition (mass, %)							
	MgO	Al_2O_3	SiO_2	CaO	TiO_2	Cr_2O_3	FeO	Total
Unaltered centre 1	13,32	15,04	0,00	0,00	0,32	48,12	26,29	103,11
Unaltered centre 2	13,65	15,72	0,17	0,15	0,40	48,52	26,01	104,62
Unaltered edge 1	12,97	13,35	0,24	0,35	0,20	49,98	26,55	103,64
Unaltered edge 2	12,43	13,11	0,28	0,15	0,30	50,74	25,75	102,76

Run no. 1/5

Position : Inner wall Equipment : SEM Total : Normalized
Sample no.: AW 607 Polaroid no.: 04114

Point description	Composition (mass, %)						
	MgO	Al_2O_3	SiO_2	CaO	TiO_2	Cr_2O_3	FeO
Altered edge 1	21,72	27,49	0,81	0,00	0,08	44,89	5,01
Altered edge 2	22,87	33,81	1,18	0,13	0,17	36,68	5,16
Altered edge 3	21,82	30,40	0,74	0,00	0,04	41,98	5,02
Altered centre	21,72	21,44	0,90	0,08	0,58	50,04	5,24
Slag crystalline 70%	24,29	15,59	54,26	0,62	0,37	1,03	3,84
Slag matrix 30%	12,64	19,67	60,17	1,99	0,38	0,82	4,34

Position : Outer wall Equipment : Probe Total : Not normalized
Sample no.: AW 607 Polaroid no.: 0096

Point description	Composition (mass, %)							
	MgO	Al_2O_3	SiO_2	CaO	TiO_2	Cr_2O_3	FeO	Total
Unaltered centre 1	10,94	15,58	0,00	0,00	0,56	46,62	25,69	99,39
Unaltered centre 2	10,74	15,38	0,02	0,00	0,42	46,63	26,04	99,26
Unaltered edge 1	10,99	15,09	0,00	0,03	0,23	45,97	26,17	98,56
Unaltered edge 2	10,95	15,00	0,04	0,00	0,24	46,36	25,43	98,04
Slag matrix 100% 1	11,39	18,03	51,40	1,16	1,40	0,59	16,46	100,62
Slag matrix 100% 2	11,33	17,71	51,70	1,20	1,20	2,35	16,18	100,07

Run no. 2/5

Position : Inner wall Equipment : SEM Total : Normalized
Sample no.: AW 606 Polaroid no.: 04111

Point description	Composition (mass, %)						
	MgO	Al_2O_3	SiO_2	CaO	TiO_2	Cr_2O_3	FeO
Altered edge 1	13,51	27,00	0,55	0,01	0,05	39,36	19,53
Altered edge 2	12,34	21,74	0,86	0,04	0,26	43,52	21,24
Altered edge 3	12,22	22,71	0,78	0,11	0,24	43,31	20,84
Altered centre	11,49	18,70	0,63	0,00	0,38	47,74	21,05
Slag matrix 100%	5,34	19,60	52,89	6,38	1,32	0,92	13,55

Position : Inner wall Equipment : Probe Total : Not normalized
Sample no.: AW 606 Polaroid no.: 0091

Point description	Composition (mass, %)							
	MgO	Al_2O_3	SiO_2	CaO	TiO_2	Cr_2O_3	FeO	Total
Unaltered centre 1	10,53	14,82	0,01	0,00	0,46	48,49	24,84	99,20
Unaltered centre 2	10,64	14,95	0,03	0,02	0,48	48,11	24,52	98,77
Unaltered edge 1	10,31	13,45	0,04	0,03	0,24	49,32	24,46	97,88
Unaltered edge 2	10,46	13,48	0,11	0,02	0,30	49,34	24,75	98,48
Slag crystalline 60% 1	21,22	11,85	46,68	0,88	2,06	1,12	12,96	101,32
Slag crystalline 60% 2	22,11	12,08	47,20	0,73	1,73	1,24	14,27	102,32
Slag matrix 40% 1	2,02	18,62	54,71	7,97	0,96	1,19	18,48	99,71
Slag matrix 40% 2	2,70	18,45	53,75	7,67	0,78	1,27	18,10	100,06

Run no. 2/5 (continued)

Position : Outer wall Equipment : SEM Total : Not normalized
Sample no.: AW 606

Point description	Composition (mass, %)							
	MgO	Al_2O_3	SiO_2	CaO	TiO_2	Cr_2O_3	FeO	Total
Unaltered centre 1	11,05	14,20	1,46	0,00	0,47	43,01	22,06	92,25
Unaltered centre 2	11,92	14,79	1,33	0,00	0,28	43,80	21,25	93,37
Unaltered edge 1	11,77	13,17	1,24	0,18	0,35	43,98	21,48	92,17
Unaltered edge 2	11,65	14,43	1,20	0,17	0,40	44,01	21,88	93,74
Slag crystalline 50% 1	22,08	11,48	47,38	0,97	1,08	0,58	17,55	101,12
Slag crystalline 50% 2	21,90	11,60	46,48	0,90	1,37	0,75	18,32	101,32
Slag matrix 50% 1	1,95	16,74	50,76	7,56	2,55	0,66	13,96	94,18
Slag matrix 50% 2	2,79	16,38	50,94	7,20	2,10	1,24	13,60	94,16

Position : Upper wall (no slag contact) Equipment : SEM Total : Not normalized
Sample no.: AW 666

Point description	Composition (mass, %)							
	MgO	Al_2O_3	SiO_2	CaO	TiO_2	Cr_2O_3	FeO	Total
Unaltered centre 1	13,45	14,92	0,00	0,17	0,40	49,41	24,35	102,70
Unaltered centre 2	12,43	14,43	0,15	0,17	0,52	48,03	24,43	100,16
Unaltered edge 1	12,33	12,58	0,13	0,20	0,10	50,79	24,74	101,17
Unaltered edge 2	11,78	12,67	0,28	0,20	0,17	49,53	23,73	98,36

Run no. 3/5

Position : Inner wall Equipment : SEM Total : Normalized
Sample no.: AW 605 Polaroid no.: 4107

Point description	Composition (mass, %)						
	MgO	Al_2O_3	SiO_2	CaO	TiO_2	Cr_2O_3	FeO
Altered edge 1	17,04	19,46	0,62	0,10	0,41	46,47	15,90
Altered edge 2	17,18	29,08	0,73	0,01	0,07	37,81	15,12
Altered edge 3	17,87	29,50	0,60	0,18	0,19	36,83	14,83
Altered centre	13,12	15,66	0,38	0,01	0,34	47,37	23,11
Slag crystalline 30%	4,92	16,05	47,90	17,31	0,49	1,13	12,20
Slag crystalline 30%	38,72	2,21	43,28	10,87	0,07	1,23	13,31
Slag matrix 40%	13,97	12,39	45,94	1,18	0,48	1,55	14,80

Position : Outer wall Equipment : Probe Total : Not normalized
Sample no.: AW 605 Polaroid no.: 0089

Point description	Composition (mass, %)							
	MgO	Al_2O_3	SiO_2	CaO	TiO_2	Cr_2O_3	FeO	Total
Unaltered centre 1	12,16	15,09	0,00	0,02	0,55	48,49	23,05	99,38
Unaltered centre 2	12,04	15,35	0,00	0,01	0,48	47,99	23,25	99,19
Unaltered edge 1	12,48	15,43	0,00	0,06	0,53	48,73	22,85	100,09
Unaltered edge 2	12,27	14,94	0,02	0,08	0,36	49,29	22,56	99,54
Slag crystalline 60% 1	8,63	12,52	41,54	18,07	1,30	0,96	14,44	97,51
Slag crystalline 60% 2	8,92	12,97	43,00	18,10	1,22	1,16	13,84	99,22
Slag matrix 40% 1	1,48	18,76	50,73	10,68	0,91	0,97	14,12	98,07
Slag matrix 40% 2	1,83	18,24	48,55	11,62	0,94	1,26	14,49	97,76

Run no. 6/5

Position : Outer wall Equipment : SEM Total : Normalized
Sample no.: AW 613 Polaroid nos: 04145 and 04144

Point description	Composition (mass, %)						
	MgO	Al_2O_3	SiO_2	CaO	TiO_2	Cr_2O_3	FeO
Unaltered centre 1	12,61	16,52	0,37	0,10	0,16	48,10	22,14
Unaltered centre 2	12,38	17,00	0,56	0,14	0,30	47,05	22,56
Unaltered edge 1	12,36	16,51	0,49	0,15	0,26	47,61	22,62
Slag crystalline 80% 1	16,78	12,05	50,47	0,76	1,00	1,65	17,29
Slag crystalline 80% 2	17,65	12,16	50,63	0,48	0,76	1,11	17,20
Slag matrix 20% 1	3,14	15,25	62,14	3,41	1,47	1,31	13,27
Slag matrix 20% 2	2,20	16,09	57,42	4,83	2,08	1,40	15,97

Position : Outer wall Equipment : SEM Total : Not normalized
Sample no.: AW 613

Point description	Composition (mass, %)							
	MgO	Al_2O_3	SiO_2	CaO	TiO_2	Cr_2O_3	FeO	Total
Unaltered centre 1	14,58	17,17	0,43	0,20	0,18	47,00	20,43	99,99
Unaltered centre 2	14,90	16,98	0,43	0,18	0,28	45,26	20,58	98,61
Unaltered edge 1	15,00	17,83	0,00	0,10	0,13	46,59	20,93	100,58
Unaltered edge 2	14,93	18,44	0,15	0,13	0,30	47,06	21,27	102,28
Slag crystalline 65% 1	25,30	13,30	51,99	0,22	0,95	0,99	15,34	108,09
Slag crystalline 65% 2	20,82	13,90	51,24	0,76	0,85	0,86	17,32	105,75
Slag matrix 35% 1	2,92	17,17	61,20	4,23	1,98	1,34	13,11	101,95
Slag matrix 35% 2	3,48	17,47	61,84	3,77	2,10	1,10	14,93	104,69

Run no. 7/5

Position : Outer wall Equipment : SEM Total : Normalized
Sample no.: AW 611 Polaroid nos: 04135 and 04134

Point description	Composition (mass, %)						
	MgO	Al_2O_3	SiO_2	CaO	TiO_2	Cr_2O_3	FeO
Unaltered centre 1	10,14	14,27	0,00	0,06	0,40	48,94	25,21
Unaltered centre 2	11,21	11,59	0,98	0,34	0,23	51,31	24,35
Unaltered edge 1	11,46	11,43	0,78	0,48	0,15	51,63	24,07
Unaltered edge 2	11,78	14,59	0,20	0,21	0,45	47,39	25,38
Slag crystalline 70%	8,38	11,69	44,38	22,16	0,91	1,20	11,27
Slag matrix 30%	0,89	16,35	49,40	12,12	0,60	3,09	17,55

Run no. 8/5

Position : Inner wall Equipment : SEM Total : Normalized
Sample no.: AW 604 Polaroid no.: 4106

Point description	Composition (mass, %)						
	MgO	Al_2O_3	SiO_2	CaO	TiO_2	Cr_2O_3	FeO
Altered edge 1	13,66	6,22	0,68	0,23	0,01	62,60	16,59
Altered edge 2	13,47	5,39	0,70	0,43	0,11	62,70	17,16
Altered edge 3	12,50	5,30	0,49	0,58	0,13	63,89	17,12
Altered centre	14,21	15,16	0,29	0,36	0,57	50,74	18,69
Slag crystalline 80%	7,86	8,29	48,06	26,64	0,50	0,75	7,91
Slag matrix 20%	0,01	9,48	48,83	37,45	0,31	0,60	3,32

Position : Outer wall Equipment : Probe Total : Not normalized
Sample no.: AW 604 Polaroid no.: 0057

Point description	Composition (mass, %)							
	MgO	Al_2O_3	SiO_2	CaO	TiO_2	Cr_2O_3	FeO	Total
Unaltered centre 1	10,79	14,86	0,00	0,09	0,48	49,00	25,03	100,28
Unaltered centre 2	10,68	14,92	0,00	0,07	0,42	48,50	24,85	99,47
Unaltered edge 1	10,43	13,03	0,00	0,21	0,14	51,43	24,27	99,54
Unaltered edge 2	10,42	12,09	0,00	0,20	0,14	51,23	24,04	99,00
Slag crystalline 60% 1	7,09	16,74	39,72	22,43	1,71	0,98	11,64	100,35
Slag crystalline 60% 2	7,72	16,57	40,08	22,74	1,53	1,10	11,55	101,32
Slag matrix 40% 1	0,18	16,82	47,53	21,82	0,44	0,65	12,48	98,48
Slag matrix 40% 2	0,21	16,93	47,99	21,59	0,43	0,88	10,36	98,94

Additional analyses to check accuracy

Position : Upper wall (no slag contact) Equipment : Probe Total : Normalized
Sample no.: AW 665

Point description	Composition (mass, %)						
	MgO	Al_2O_3	SiO_2	CaO	TiO_2	Cr_2O_3	FeO
Unaltered centre *	11,15	13,12	0,01	0,00	0,23	48,93	26,45
Unaltered edge *	11,41	12,96	0,00	0,00	0,25	48,14	26,00

* Mean of four determinations

Run no.: 6/4

Position : Outer wall Equipment : SEM Total : Normalized
Sample no.: AW 612

Point description	Composition (mass, %)						
	MgO	Al_2O_3	SiO_2	CaO	TiO_2	Cr_2O_3	FeO
Unaltered centre	10,01	10,80	0,00	0,02	0,11	51,12	27,94
Unaltered edge	10,29	10,78	0,00	0,07	0,10	51,23	27,52
Slag crystalline 20%	15,95	7,81	50,82	8,58	0,09	0,96	15,80
Slag matrix 80%	0,89	13,80	50,62	9,35	0,09	0,70	24,52

REFERENCES

1. GRAF, H., and EICH, G. 75 years of stainless steel. Stahl Eisen (1987), vol. 107. pp. 21-29.
2. SIMMONS, R.P. A bright future for stainless steel. Iron and Steelmaker (March, 1985). pp. 27-30.
3. VOLKERT, G., and FRANK, K.D. (ed.). Metallurgie der ferrolegierungen. 2nd Ed. Springer-Verlag. Berlin (1972).
4. SLATTER, D., et al. Technology for the production of new grades and types of ferro-alloys using thermal plasma. INFACON '86, 4th Int. Ferro-alloy Congress, Sao Paulo. Associacao Brazileira dos Productores de Ferro-Ligas (ABRAFE), Sept. 1986. 10 pp.
5. KUWABARA, M., et al. Influence of main factors on the reaction (Production of ferro-chrome by the smelting reduction in a stirred bath - I). Trans. ISIJ., vol. 24, (1984). p B-378.
6. OOSTHUYZEN, E.J., and VILJOEN, E.A. Quantitative mineralogy applied to a study of the process involved in the production of ferrochromium from Transvaal chromite ore. Proc. XIV Int. Mineral Processing Congress, Toronto, Canadian Institute of Metallurgy (1982). pp. VIII 6.1-6.17.
7. BARCZA, N.A., et al. Recent developments in the ferro-alloy field in South Africa. Proceedings, 12th Congress of the Council of Mining and Metallurgical Institutions. Gelen, H.W. (ed.). Johannesburg, The S.A. Institute of Mining and Metallurgy, 1982, vol. 2. pp. 595-604.

8. BARCZA, N.A., et al. The production of ferrochromium in a transferred-arc plasma furnace. 39th Electric Furnace Conf. Proc., Houston, Iron and Steel Society of the AIME, 1982. pp. 243-260.

9. ENOKIDO, T., et al. Influence of slag composition and reaction mechanism (Production of ferro-chrome by the smelting-reduction in a stirred bath - II). Trans. ISIJ. vol. 24, (1984). p. B.-379.

10. KUWABARA, M. Smelting reduction of 20% chromium molten iron with 650 kg top and bottom blowing converter (Production of ferro-chrome by the smelting reduction in a stirred bath -III). Trans. ISIJ, vol. 24 (1984). p. B.380.

11. LEVIN, E.M., et al. Phase diagrams for ceramists. 2nd Ed. The American Ceramic Society, Columbus, Ohio, 1964.

12. HEALY, G.W. The thermodynamics of chromite ore smelting. Iron and Steelmaker, Dec. 1987. pp. 51-59.

13. ULMER, G.C. Chromite spinels in high temperature oxides. vol. 5, Part I. Ed. A.M. Alper. Academic Press, N.Y., 1970. pp. 255-314.

14. BURNS, R.G. Crystal field effects in chromium and its partitioning in the mantle. Geochimica et Cosmochimica Acta, (1975), vol. 39. pp. 857-864.

15. ULMER, G.C. Oxidation-reduction reactions and equilibrium phase relations at 1300°C at oxygen pressures from 0,21 to 10^{-14} atmospheres for the spinel solid solution series $FeCr_2O_4$-$MgCr_2O_4$ and $FeAl_2O_4$-$MgAl_2O_4$. PhD Thesis, Pennsylvania State University, (1964).

16. DATTA, R.K. Order-disorder in spinels. PhD Thesis, Pennsylvania State University, (1961).

17. STUBICAN, V.S., and GRESKOVICH, C. Trivalent and divalent chromium ions in spinels. Geochimica et Cosmochimica Acta, (1975), vol. 39. pp. 875-881.

18. BARCZA, N.A. Mass and energy balances on ferrochromium smelting furnaces. Private Communication, 1979.

19. RANKIN, W.J., and BISWAS, A.K. Oxidation states of chromium in slags and chromium distribution in slag-metal systems at 1600°C. J. Inst. of Mining and Metallurgy, (Mar. 1978). pp. C60-C70.

20. MAEDA, M. and SANO, N. Thermodynamics of chromium oxide in molten $CaO-MgO-Al_2O_3-SiO_2$ slags coexisting with solid carbon. Tetsu-to-Hagane, vol. 68, (1982). pp. 759-766.

21. MUAN, A. Equilibria in metal and oxide systems at high temperatures. Spec. Publ. Geol. Soc. S.Afr., vol. 7, (1983). pp. 325-336.

22. KOERBER, F., and OELSEN, W. The reactions of chromium with acid slags. Mitt. Kais.-Wilh.-Inst. Eisenforschung, Dusseldorf, (1935), vol. 17. pp. 231-245.

23. ESIN, O.A., and ZAKHAROV, D.I.N. Solubility of chromium oxides in molten slags in contact with the metal. Bull. Inst. Higher Education - Ferrous Metallurgy, USSR, no. 11. (1958). pp. 45-52.

24. BARIN, I., and KNACKE, O. Thermodynamical properties of inorganic substances. Springer-Verlag, Berlin, 1973.

25. TOKER, N.Y. Equilibrium phase relations and thermodynamics for the systems Cr-O and Fe-Cr-O in the

temperature range 1500°C to 1820°C. PhD Thesis. Pennsylvania State University, 1978.

26. HEALY, G.W. Activities in the liquid Cr-Fe-C system above 1600°C. Reinhardt Schuhmann Int. Symp. Trans. Metallurgical Soc. of AIME, Colorado Springs, (Nov. 1986). pp. 667-679.

27. BARCZA, N.A. Incipient fusion studies in the system Chromite-CaO-MgO-Al_2O_3-SiO_2-C. M.Sc Thesis. University of the Witwatersrand (1971).

28. BARNES, A.R., and FINN, C.W.P. The prereduction of chromite from the UG-2 reef. Randburg, Council for Mineral Technology, NIM Report 2070, (Oct. 1980). 24 pp.

29. SEARLE. M.J., and FINN, C.W.P. The mathematical modelling of the reduction behaviour of chromite from the upper chromitite layer of the Bushveld Complex. Randburg, Council for Mineral Technology, Report M96, (Jul. 1983). 26 pp.

30. ALGIE, S.H., and FINN, C.W.P. Reaction mechanisms in the reduction of Winterveld chrome spinel with graphite and carbon. Randburg, Council for Mineral Technology, Report M157, (Dec. 1984). 49 pp.

31. URQUHART, R.C. Reactions occurring during the smelting of high-carbon ferrochromium from Transvaal chromite ores. Randburg, Council for Mineral Technology, NIM Report 1482, (Apr. 1973). 31 pp.

32. DAWSON, N.F., and EDWARDS, R.I. Factors affecting the reduction rate of chromite. Proc. INFACON '86. 4th Int. Ferro-alloy Congress, Sao Paulo, Associacao

Brasileira dos Productores de Ferro-Ligas (ABRAFE), (Sept. 1986). 7 pp.

33. FUKAGAWA, S., and SHIMODA, T. Smelting reduction mechanism of chromium ore sinter by solid carbon. Trans. ISIJ, vol. 27, (1987). pp. 609-617.

34. ROBISON, J.W., and PEHLKE, R.D. Kinetics of chromium oxide reduction from a basic steelmaking slag by silicon dissolved in liquid iron. Met. Trans., vol. 5, (May 1974). pp. 1042-1051.

35. ELLIOTT, J.F., and GLEISER, M. Thermochemistry for steelmaking. Vol. 1. Addison-Wesley, Massachusetts, USA, 1960.

36. ROOS, E.H. Measurement of the rate of dissolution of chromite by the use of the rotating cylinder technique. M.Sc. Thesis. University of the Witwatersrand, 1981.

37. DE WAAL, S.A., and HIEMSTRA, S.A. The mineralogy, chemistry and certain aspects of reactivity of chromitite from the Bushveld Igneous Complex. Johannesburg, Council for Mineral Technology. NIM Report 1709, (1975). 86 pp.

38. British Standards Institution. B.S. 1902, Part 1A. Determination of density and porosity, (1966).

39. COOPER, R.A., and WEEKES, A.J. Data, models and statistical analysis. Philip Allan, Deddington, UK, (1983). pp. 91-103.

40. HUYN, D-B., and SHIM, J-D. Application of the subregular solution model in evaluating activity of iron-oxide in steelmaking slags. Trans. ISIJ, vol. 28, (1988). pp. 736-745.

41. KEITH, M.L. Phase equilibria in the system $MgO-Cr_2O_3-SiO_2$. J. Amer. Ceram. Soc., vol. 37 (1945). pp. 490-496.

42. GEIGER, G.H., and POIRIER, D.R. Transport phenomena in metallurgy. Addison-Wesley, Menlo Park, California, 1973. p. 525.

43. SIGWORTH, G.K., and ELLIOTT, J.F. The thermodynamics of liquid dilute iron alloys. Metal Sci., vol. 8, (1974). pp. 298-310.

44. FINN. C.W.P. Design criteria for molybdenum windings. Private Communication, 1984.

45. BOCKRIS, J.O.M. General aspects of physiochemical research at high temperatures. Butterworths Scientific Publications, London, 1959.

Author: Curr, Thomas Robert.
Name of thesis: The Dissolution Of A Transvaal Chromite In Liquid Silicate Slags Under An Inert Atmosphere At 1550 Celcius Degrees And 1650 Celsius Degrees.

PUBLISHER:
University of the Witwatersrand, Johannesburg
©2015

LEGALNOTICES:

Copyright Notice: All materials on the University of the Witwatersrand, Johannesburg Library website are protected by South African copyright law and may not be distributed, transmitted, displayed or otherwise published in any format, without the prior written permission of the copyright owner.

Disclaimer and Terms of Use: Provided that you maintain all copyright and other notices contained therein, you may download material (one machine readable copy and one print copy per page)for your personal and/or educational non-commercial use only.

The University of the Witwatersrand, Johannesburg, is not responsible for any errors or omissions and excludes any and all liability for any errors in or omissions from the information on the Library website.